Paleobiology, 30(3), 2004, pp. 444–470

Morphometric analysis of humerus and femur shape in Morrison sauropods: implications for functional morphology and paleobiology

Matthew F. Bonnan

Abstract.—Morphometric analyses of sauropod limbs have the potential to illuminate functional aspects of sauropod locomotion and paleobiology. However, analyses of sauropod limb dimensions typically show few discernible morphological trends because of large size differences among the individuals in a sample. For sauropods, combined analyses of both limb dimension and shape may be more desirable. Numerous humeri and femora from *Apatosaurus*, *Diplodocus*, and *Camarasaurus* provide an opportunity to explore and compare limb morphology in contemporaneous, sympatric sauropods. Thin-plate splines were used to analyze landmark-based shape differences in combination with traditional morphometrics. The aims of the analysis were (1) to determine if humerus and femur shape were significantly different among the genera; (2) to determine where shape changes occurred; and (3) to infer the basic functional implications of the shape differences using an Extant Phylogenetic Bracket approach. Few differences were detected among the genera using traditional morphometric analyses, and linear regression revealed a predominantly isometric relationship between most measurement variables and element size. Thin-plate splines revealed significant shape differences among the taxa. *Apatosaurus* humeri and femora were the most robust, with expanded regions for muscle insertion and more distally placed deltopectoral and caudofemoral landmarks. *Diplodocus* humeri and femora were gracile, with more proximally located landmarks of muscular insertion. *Camarasaurus* humeri were surprisingly gracile, with a less extensive deltopectoral crest, but had more robust femora similar to those of *Apatosaurus*. Few differences distinguished juvenile from adult specimens. These data suggest some locomotor differences were present among the three genera.

Matthew F. Bonnan. Department of Biological Sciences, Western Illinois University, Macomb, Illinois 61455. E-mail: MF-Bonnan@wiu.edu

Accepted: 11 November 2003

Introduction

Both qualitative and quantitative analyses of bone shape continue to play a central role in the evaluation of dinosaur evolution and paleobiology (Chapman and Weishampel 1997a,b). Appendicular synapomorphies related to locomotor adaptations form a majority of the characters on which dinosaur evolution and phylogeny have been established (Benton 1997; Sereno 1999), and the relationship between limb morphology and locomotor performance has long been explored in many saurischian and ornithischian taxa. Because locomotion is the result of a complex series of interactions among bones, their soft tissues, and a substrate, simplification of these factors for the purposes of discovering broad evolutionary or functional trends has been the goal of most morphometric studies on dinosaurs. Recognition of a link between limb proportions and general locomotor performance (Alexander and Jayes 1983; Alexander 1989; Hildebrand and Goslow 2001) has spawned a proliferation of morphometric studies that use limb dimensions, limb segment lengths, and ratios to elucidate locomotor categories and trends among major dinosaur clades (e.g., Coombs 1978; Alexander 1989; Thulborn 1989; Lehman 1990; Weishampel and Chapman 1990; Foster 1995; Carrano 1997, 1998, 1999; Chapman 1997; Curtice et al. 1997; Gatesy and Middleton 1997; Farlow et al. 2000; Jones et al. 2000).

Few morphometric studies have focused on sauropod dinosaur limb elements. Analysis of sauropod limbs inherently suffers from difficulties related to size, size differences among individuals, and poor taxonomic samples, all of which may account for the general paucity of morphometric studies on these dinosaurs. Sauropod limbs have the disadvantage of being large, massive, and fragile, and this in itself poses problems for data collection (e.g.,

 0094-8373/04/3003-0006/$1.00

one cannot easily access all sides of a limb bone). However, interpretation of morphometric signals is by far the most problematic. For example, differences in the size of limb elements between juvenile or subadult sauropods and those of adults, or between taxa of differing size, are so great that size alone accounts for almost all variation in a particular sample. This is reflected in the results from the few previous preliminary (Foster 1995; Curtice et al. 1997; Wilhite and Curtice 1998; Wilhite 1999) and published (Christiansen 1997) morphometric analyses of sauropod limbs. These show collectively that most differences in limb dimensions among sauropod taxa and individuals are size-related with weak allometric signals. Despite these difficulties, morphometric analyses of sauropod limbs have the potential to illuminate evolutionary and functional trends. In spite of their size, the broad geographic distribution of several North American Late Jurassic taxa (e.g., *Apatosaurus*, *Diplodocus*, *Camarasaurus*) (McIntosh 1990; Dodson 1990; McIntosh et al. 1997) suggests that at least some of these dinosaurs were quite vagile animals. Quantitative assessment of bone shape may augment functional interpretations of locomotion or identify morphological differences among contemporaneous taxa. Moreover, many synapomorphies rooted in appendicular skeleton morphology are used to chart sauropod evolutionary history (Upchurch 1995, 1998; Wilson and Sereno 1998; Wilson 2002).

Most of the morphometric analyses published on dinosaur postcrania implicitly assume that linear measurements of bone dimensions and maxima accurately capture bone shape. Undoubtedly, significant allometric relationships and trends have been shown for many dinosaur taxa using linear distance measures, and these results have provided the empirical data necessary for interpreting the broad evolutionary trends of locomotion in various dinosaur clades. However, such data do not capture or reflect shape information per se. Analysis of the linear dimensions of sauropod limbs, where size discrepancies between and among specimens are great, may mask potential shape information. Statistical techniques that examine shape, instead of size-dependent linear measurements, have recently come into use (Bookstein 1990, 1991, 1996; Chapman 1990a,b, 1997; Rohlf and Slice 1990; Rohlf 1993, 1998; MacLeod 1999). One particular shape analysis technique, thin-plate splines, has proved valuable in studies of both extant and fossil mammalian taxa (Swiderski 1993; Zelditch et al. 1995; Birch 1997; Monterio 1999). Thin-plate splines evaluate shape differences among a set of objects, such as bones, by comparing homologous landmarks among all specimens in a sample to a generalized, grand mean form (Bookstein 1991; Rohlf 1993). As all digitized objects are size standardized through mathematical derivation, the technique is ideal for analyzing bone shape (rather than bone dimension) as well as providing both qualitative visualizations of bone shape change and quantitative components called partial and relative warps (Bookstein 1991, 1996; Rohlf 1993; Birch 1997).

Three sympatric Late Jurassic neosauropods (*Apatosaurus*, *Diplodocus*, *Camarasaurus*) occur contemporaneously throughout the Morrison Formation (Dodson et al. 1980; Dodson 1990) and perhaps competed with one another for vegetative resources. Morphological differences in their skulls and teeth (Fiorillo 1991; Calvo 1994; Upchurch and Barrett 2000), as well as their cervical mobility and range (e.g., Dodson 1990; Stevens and Parrish 1999; Upchurch and Barrett 2000), have previously been examined and compared in these three genera. However, comparisons of limb morphology among the three remain limited and largely qualitative. The numerous humeri and femora of the three genera provide a rare opportunity to explore morphometric limb variation among large, sympatric dinosaurian herbivores. Using a combination of traditional morphometric approaches and thin-plate splines, the present study aims (1) to determine whether statistically significant morphological differences occur among *Apatosaurus*, *Diplodocus*, and *Camarasaurus* humeri and femora; (2) to establish where shape differences associated with anatomical landmarks and regions occur in the humeri and femora; and (3) to use an Extant Phylogenetic Bracket approach to infer the functional implications of

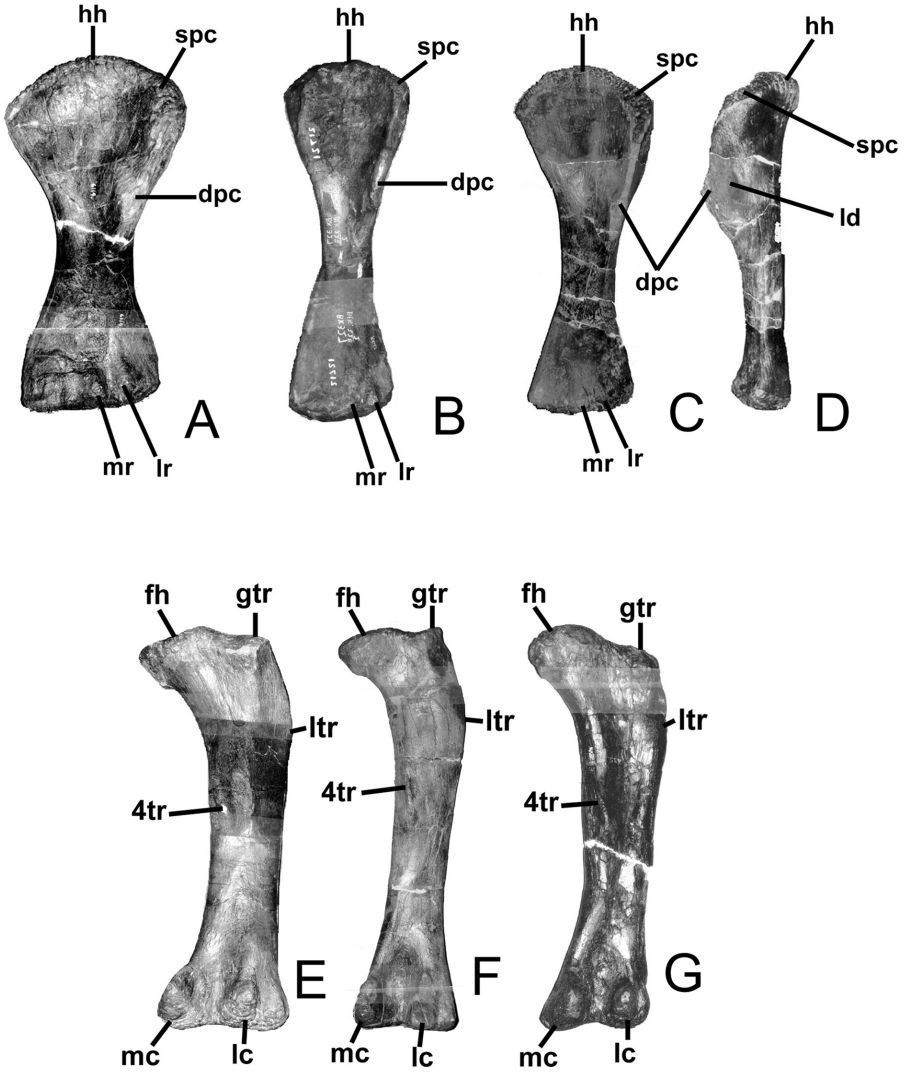

FIGURE 1. Representative humeri and femora of *Apatosaurus* (A [AMNH 6114], E [BYU Display]), *Diplodocus* (B [CM 21721], F [AMNH 5855]), and *Camarasaurus* (C,D [MWC Display], G [AMNH 435]). All humeri are shown in anterior view, except D, which is a lateral view, and all femora are shown in posterior view. Not to scale. Abbreviations: 4tr, fourth trochanter; dpc, deltopectoral crest; fh, femoral head; gtr, greater trochanter; hh, humeral head; lc, lateral condyle; ld, inferred insertion of M. latissimus dorsi; lr, lateral ridge; ltr, lesser trochanter; mc, medial condyle; mr, medial ridge; spc, proximal extent of deltopectoral crest and inferred insertion site of M. supracoracoideus.

humeral and femoral shape differences among the genera.

Materials and Methods

Specimens and Measurement.—The humeri and femora of *Apatosaurus*, *Diplodocus*, and *Camarasaurus* were examined at 14 North American collections (Fig. 1) (see Appendix 1 for repository information; measurements available in Bonnan 2001). Humeri and femora were selected for analysis because these appendicular elements are the most abundant in North American collections and provide the largest sample size for statistical tests. Other sauropod limb elements (especially ulnae, radii, and fibulae) have exceedingly simple morphologies with few discernible landmarks, characteristics that make them more difficult to digitize for shape analysis (Bonnan 2001). Tibiae were difficult to digitize because their morphology does not translate well to a two-dimensional analysis (see Bonnan 2001 for

more details). As discussed above, these three taxa were selected because of their probable sympatric and paleoecological associations in Morrison Formation assemblages (Dodson 1990). Contemporaneous sauropod taxa of the Tendagaru provide another well-represented sample of appendicular elements (Dodson 1990). However, examination of these taxa is beyond the scope of the present analysis and will constitute a separate study (Bonnan unpublished data).

Taxonomic identifications of most humeri and femora were based on their association with other skeletal elements or, in some cases (e.g., *Apatosaurus louisae* [CM 3018]), were made from nearly complete specimens. No unidentified or questionable elements were included in the analysis. For isolated humeri and femora, the element's generic identity was established by using identifications, figures, and descriptions of complete or nearly complete skeletons published by Ostrom and McIntosh (1966) and McIntosh (1990). In no case was there a contradiction between the isolated element's identification and the basic descriptions of that element from more complete material. For a comprehensive review of Morrison sauropod appendicular material, see Wilhite 2003.

Standardized measurements were taken on the humeri and femora (Fig. 2) with measuring tape to the nearest centimeter (±1 cm) and are reported here in millimeters (see Appendix 2 for variable abbreviations). A subsample of the humeri and femora was photographed for thin-plate splines digitization. Controlled photography of each element in a specific orientation can be difficult because many elements will be fixed in skeletal mounts and some will be damaged. As much as possible, selection of the elements to be digitized was based on the following criteria: (1) a photograph or series of photographs could be taken of the element in which the morphological features of interest lay on a contour parallel to the plane of the camera lens; and (2) a standardized, photographic position of the element lying naturally on the floor was possible without extensive propping or elevation of certain morphological aspects relative to others. Humeri were photographed lying on a flat surface, their anterior faces exposed, whereas femora were photographed lying on a flat surface, their posterior faces exposed (Fig. 3). Photographs were taken with a standard 35-mm camera mounted on a tripod over the bone of interest at a predetermined, standardized height of 1850 mm. The tripod was leveled by using a built in bubble level, and a separate level was used on the camera itself, to en-

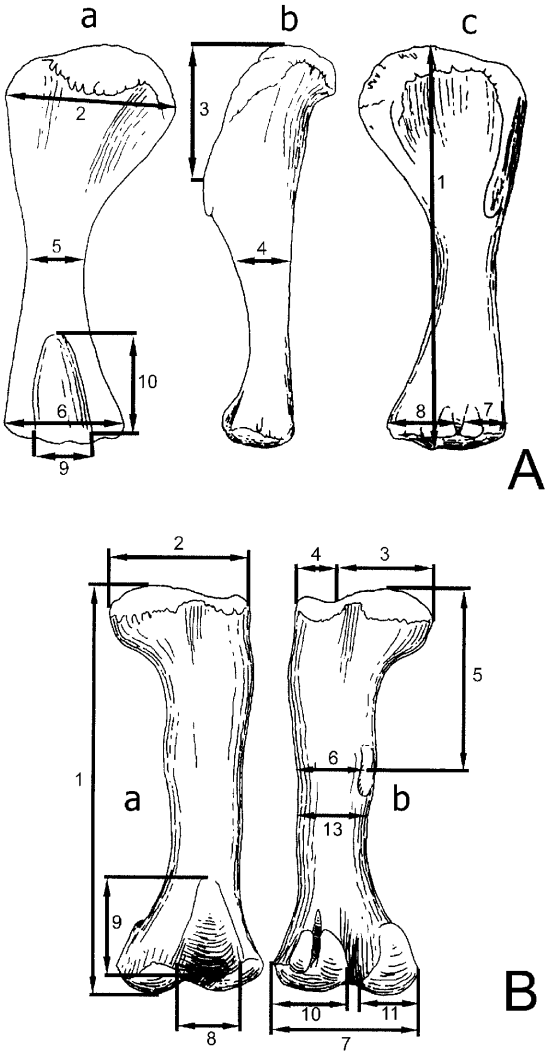

FIGURE 2. Measurement system for selected sauropod limb elements. For the femur where the anteroposterior midshaft width measurement is not pictured, the measurement is taken perpendicular to that of mediolateral midshaft width. Line drawings modified after Ostrom and McIntosh 1966. A, Left humerus in posterior (a), lateral (b), and anterior (c) views. B, Left femur in anterior (a) and posterior (b) views. Arabic numerals refer to measurement variables listed in the appendix.

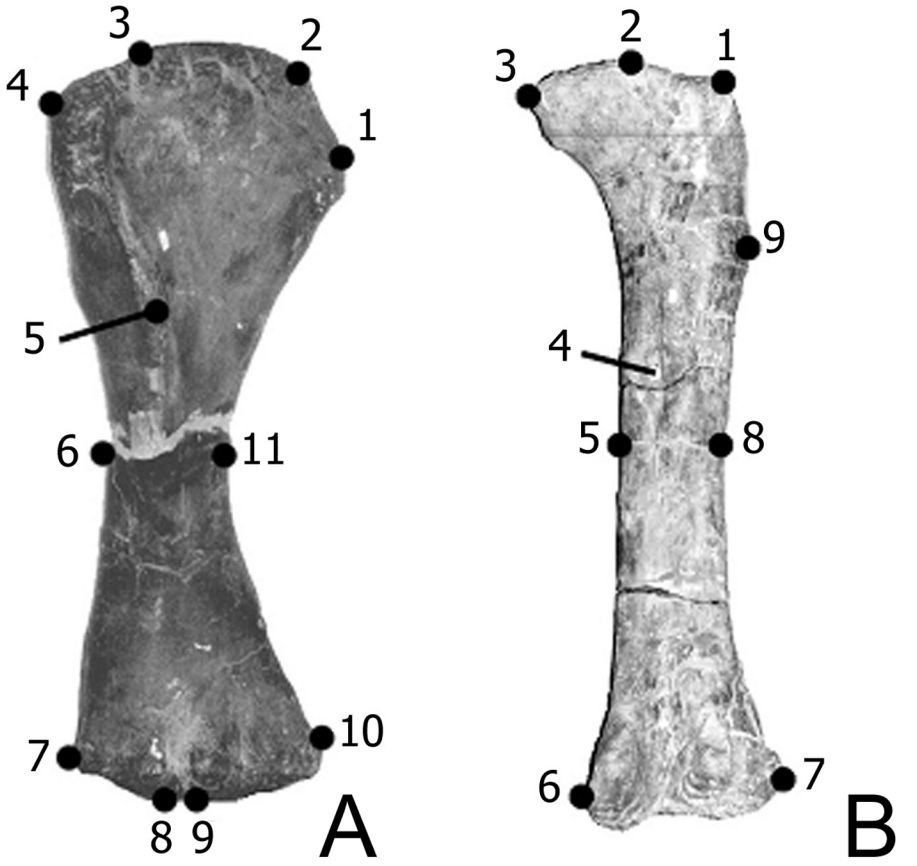

FIGURE 3. Landmarks used in thin-plate splines on sauropod humerus and femur. A, Right humerus in anterior view showing medial border of proximal humerus (1), extent of humeral head (2, 3), proximal deltopectoral crest (4), distal deltopectoral crest (5), lateral constriction of humerus (6), lateral ''epicondyle'' (7), lateral ''condyle'' (8), medial ''condyle'' (9), medial ''epicondyle'' (10), and medial constriction of the humerus (11). B, Right femur in posterior view showing greater trochanter (1), extent of femoral head (2, 3), fourth trochanter (4), medial constriction of femur shaft (5), medial condyle (6), lateral condyle (7), lateral constriction of femur shaft (8), and lateral rugosity (9).

sure as little distortion of the image as possible. Each element was then centered in the lens to decrease distortion from lens curvature or parallax. The resulting photographs were then scanned on a flatbed scanner, cropped, scaled to a height of 5.08 cm, and digitized (see below for digitization details).

Paleobiological Inferences.—Morphometric data in this study are used to infer basic muscle changes associated with anatomical landmarks, or with regions between landmarks, in *Apatosaurus*, *Diplodocus*, and *Camarasaurus*. The successful application of any morphometric method for inferring paleobiological constraints on fossil vertebrates is ultimately tied to the interpretation of bone morphology in light of known or probable soft tissue parameters. Functional inferences reported here follow the Extant Phylogenetic Bracket method (EPB) (Witmer 1995), rooting soft tissue comparisons in an established phylogenetic framework of extant outgroup taxa. A detailed functional analysis is beyond the scope of this study, although dissection of *Alligator mississippiensis* and *Columba livia* specimens was performed to confirm the gross correlations between landmarks and soft tissue reported here (see Bonnan 2001). To simplify the present analysis, only generalized inferences of muscle function derived from Level I soft tissue inferences (Witmer 1995), or one-to-one correlations of landmarks and their soft tissues are considered. In other words, the functional inferences that are described here are

based on unequivocal, shared landmark-tissue associations by the extant bracketing taxa (crocodilians, avians) and a further removed extant outgroup (lepidosaurs). For example, it is recognized that the deltopectoral crest of the humerus is a landmark correlated with deltoid and pectoral musculature in all these taxa (Romer 1956; Hildebrand and Goslow 2001). Therefore, differences in deltopectoral crest shape among the sauropod taxa are inferred to be associated with differences in deltopectoral muscle placement and distribution along this landmark.

Functional inferences drawn from EPB associations are two levels removed from the osteology (as per the inference pyramid [Witmer 1995]). Moreover, for simplicity, gross muscle function is being inferred without a detailed consideration of other soft tissue parameters (e.g., cartilage, ligaments). As with all complex systems, however, simplifying the number of variables under consideration can be beneficial for inferring functional morphology provided that certain assumptions and limitations are acknowledged a priori and respected throughout the analysis. This study assumes: (1) that sauropod humeri and femora were loaded vertically and followed a parasagittal arc of movement during locomotion, according to simple biomechanical principles and comparisons with other graviportal vertebrates (Bonnan 2001, 2003); (2) that long-axis rotation and abduction of the humerus and femur were very restricted, judging from the shapes of their articular surfaces and those of their respective girdles (Bonnan 2001, 2003); (3) that the action of most muscles pulling on the humerus or femur would be restricted mostly to extension or flexion in a parasagittal plane; and (4) that because the humerus and femur were loaded vertically and restricted largely to a parasagittal plane of movement, missing data on joint cartilage morphology and other soft tissues will not affect the generalized interpretations of the column-like movements reported here (see Bonnan 2003 for a more detailed consideration of this issue). The functional inferences presented in the discussion are constrained by these four assumptions.

Statistical Methods.—All plots and statistical analyses were carried out on the SPSS statistical package, with the exception of the data generated by the thin-plate splines software discussed below. Linear measurement variables (but not thin-plate splines variables) were standardized through natural log transformation prior to plotting or statistical analysis (see Bookstein et al. 1985 and Bookstein 1991). The partial and relative warps were not natural-log transformed because they are already normalized through Procrustes superimposition methods (see Bookstein 1991, 1996). All linear measurement data sets were tested for normal distribution with the Shapiro-Wilk statistical procedure. Each element was analyzed with a principal components analysis (PCA), linear regression, nonparametric Kruskal-Wallace (KW) tests, and thin-plate splines.

Each PCA was conducted with a variance/covariance matrix of natural log-transformed data, and the subsequent variable loadings and bivariate plots of the principal components (PCs) were analyzed for morphometric patterns. Slopes of the natural-log-transformed variables were computed by using the standard allometric equation ($\ln y = b_0 \ln x + \ln b_1$, where b_0 is the y-intercept and b_1 is the slope; see Jolicoeur 1963 and Shea 1985 for overviews). Maximum length was selected as the independent variable. The resulting slopes were tested with a two-tailed *t*-test to determine if they differed significantly ($\alpha = 0.05$) from zero or one (i.e., isometry). As the linear measurement data were obtained from a fossil ''population,'' one cannot assume random sampling, normal distribution, and homogeneity of variances, requirements for ANOVA and MANOVA (Stevens 1996). To circumvent inevitable power reduction and increased Type I errors (see Stevens 1996), the nonparametric KW test was selected because it analyzes the distribution of the variates rather than a mean (Stevens 1996). Therefore, KW is less affected by non-normal distributions or heteroscedasticity. The KW test simply assigns ranks to the variables in each taxon, and these ranks are analyzed to determine significant differences. Significant results were evaluated with the pair-wise Mann-Whitney *U* statistic to determine which genera differed

significantly from one another. Although long series of pairwise tests can greatly decrease statistical power and increase the probability of Type I errors (see Stevens 1996), only three genera were evaluated here. Therefore, the standard error value ($\alpha = 0.05$) was divided by three ($\alpha = 0.0167$) for each test to correct for loss of statistical power.

To evaluate limb morphology through landmark-based data, I analyzed the partial and relative warps produced through decomposition of thin-plate splines (Bookstein 1991). A series of anatomically homologous landmarks were digitized on the humeri and femora in the TPSDIG (Rohlf 1997a) program. Four landmarks selected for analysis were geometrically but not strictly anatomically homologous (humerus: 6, 11; femur: 5, 8—midshaft least breadth). As many morphometric analyses use both geometric and biological landmarks (see MacLeod 2002 for a recent overview of these differences in a phylogenetic context), and as the present study is not using landmark differences to establish phylogenetic relationships, I did not anticipate that the incorporation of geometrically homologous landmarks would be problematic. The digitized landmarks serve as scaffolding for shape comparison. The program TPSRW (Rohlf 1997b) performed the partial and relative warps analyses on the digitized landmark data. All digitized elements were first averaged into a grand mean reference shape through generalized least-squares (GLS) Procrustes superimposition methods described in detail by Chapman (1990a) and Bookstein (1991, 1996). The reference form is nonlocal and nonarbitrary (Rohlf and Slice 1990; Bookstein 1996), meaning its generation is not guided by any preconceived notions of best fit (e.g., RFTRA) or morphological significance. This distinction is important because the reference specimen has no phylogenetic or ontogenetic meaning but serves instead as a standard to which all other specimen shapes are compared (Bookstein 1991, 1996).

Differences in the coordinate distances of the reference form's landmarks and those of each specimen warp or bend the thin-plate spline into shapes that are visualized qualitatively, while generating quantitative variables called partial and relative warps (Bookstein 1991). Partial warps are a series of variables that describe uniform and nonuniform shape changes in an element. A single uniform component (reported as an x-y coordinate pair) is generated that describes parallel changes in element shape, whereas several non-uniform partial warps (also reported in x-y coordinate pairs) are generated in order of most localized shape changes to more general, overall changes in form. As partial warps are correlated, normalized variables that collectively describe shape change, a MANOVA was used to detect the group mean differences reported here (as per Bookstein 1996). However, the biological significance of partial warps is problematic and complex (Rohlf 1998; Zelditch et al. 1998) and has led to controversy over their implementation and interpretation in morphometric studies (e.g., Zelditch et al. 1995, 1998; Rohlf 1998). Instead, relative warps are examined to extract biologically meaningful patterns of total shape change (Rohlf 1993; Bookstein 1996; Birch 1997).

Relative warps are principal components of shape change derived from the covariance matrix of partial warp scores. They are uncorrelated (orthogonal) and contain almost all of the variability within a given sample (Bookstein 1996; Birch 1997; Rohlf 1997b). As with PCA, relative warp (RW) 1 describes most of the cumulative sample variation, RW 2 describes most of the remaining cumulative sample variation, and so on. The major departure from PCA is that relative warps are principal coordinates of shape variation that are derived ultimately through Procrustes superimposition methods (Bookstein 1996; Birch 1997; Rohlf 1997b). Therefore, the sample variation accounted for by the RWs is related to shape differences instead of linear dimensional measurements. Relative warps can be analyzed in several ways including various methods of data shearing, weighting, and the exclusion of uniform shape change components (see Rohlf 1993 and Bookstein 1996 for overviews). Here, relative warps were computed within the so-called total shape space (Bookstein's $\alpha = 0$) to simplify the analysis and to examine global, local, uniform, and non-uniform changes in bone shape simultaneously

TABLE 1. PCA results for the humerus. The percentage of variance is printed below each component. Variables defined in Appendix 2.

Variable	Normality p	PC 1 92.40%	PC 2 2.452%	PC 3 1.921%	PC 4 1.504%
H1	0.000	0.986	0.042	0.069	−0.082
H2	0.002	0.983	0.116	−0.068	0.023
H3	0.001	0.975	0.057	0.015	−0.109
H4	0.051	0.914	0.089	0.369	0.112
H5	0.003	0.984	0.101	−0.108	−0.012
H6	0.003	0.987	0.071	−0.024	0.064
H7	0.222	0.942	−0.004	−0.184	0.260
H8	0.001	0.978	0.064	0.016	−0.060
H9	0.012	0.909	−0.409	0.046	0.038
H10	0.002	0.957	−0.084	−0.084	−0.206

TABLE 2. PCA results for the femur. The percentage of variance is printed below each component. Variables defined in Appendix 2.

Variable	Normality p	PC 1 85.339%	PC 2 3.122%	PC 3 3.327%	PC 4 1.975%
F1	0.204	0.970	−0.122	−0.010	0.118
F2	0.165	0.978	−0.130	−0.016	−0.002
F3	0.461	0.968	0.014	−0.036	0.120
F4	0.038	0.874	−0.378	0.047	−0.280
F5	0.198	0.967	−0.111	−0.024	0.145
F6	0.674	0.931	0.023	−0.203	0.199
F7	0.509	0.973	−0.090	0.076	−0.054
F8	0.851	0.925	0.143	−0.189	−0.100
F9	0.367	0.894	0.200	−0.222	−0.105
F10	0.379	0.892	0.330	0.115	−0.190
F11	0.356	0.831	0.152	0.444	0.111
F12	0.243	0.825	0.093	0.282	0.129
F13	0.489	0.962	−0.098	0.078	0.008

(see Bookstein 1991, 1996 for more details). Shape changes reported by the relative warps were compared with the MANOVA results of the uniform and partial warp scores. An extensive literature exists on the application of thin-plate splines, and the reader is referred to Bookstein 1991, 1996 (and references therein) and Birch 1997 (provides a comparative example of the method) for more detailed procedural and statistical information.

Results

Traditional Morphometric Results

Forty-two humeri and 40 femora were measured for traditional morphometric analysis (humerus/femur: *Apatosaurus* [$n = 15/12$]; *Diplodocus* [$n = 9/11$]; *Camarasaurus* [$n = 18/17$]). Shapiro-Wilk results indicate that most humerus variables have a non-normal distribution (Table 1), whereas most femoral variables show normal distribution (Table 2). In both PCAs, four principal components were extracted. The overwhelming proportion of sample variation accounted for by PC 1 (humerus = 92%; femur = 85%) and the high positive loadings of all variables on this factor in both analyses suggest it is a size component (Tables 1, 2). Such results were expected and support previous analyses that suggest most limb variation in sauropods is accounted for by size differences. Interpreting the other components in both analyses was difficult, and few discernible patterns appear in the plots of the components or variables (see below). Refer to Figure 4 for plots of the humerus and Figure 5 for plots of the femur. Variable abbreviations (see Appendix 2) are included next to the variable names in the text to facilitate comparison with table data.

Humerus Results.—Nine incomplete specimens were excluded from the PCA. Variable loadings suggest PC 2 is a component of olecranon fossa breadth (H9), PC 3 is anteroposterior midshaft width (H4), and PC 4 is a contrast of lateral condyle breadth (H7) with olecranon fossa height (H10) (Table 1). Together, these three PCs account for less than 6% of the total sample variation. All PCA plots show little else but size-related distributions: specimens plot in order of size along PC 1, and the four *Apatosaurus* specimens clustered at the negative end of the PC 1 axis are juveniles. No significant differences were reported among the three genera on any of the variables using the KW test. Few distinct allometric trends were present in most bivariate plots, and regression of humerus variables against maximum length consistently produced nearly isometric slopes not significantly different from one for most variables (Table 3). Certain humeral dimensions have moderately negative allometric slopes ($b_1 \cong 0.6354$–0.8420) in *Camarasaurus* (proximal and distal breadth [H2, H6], mediolateral midshaft width [H5], medial ''condyle'' breadth [H8], and olecranon fossa dimensions [H9, H10]). These results suggest that mediolateral and olecranon fossa expansion lag slightly behind an increase in

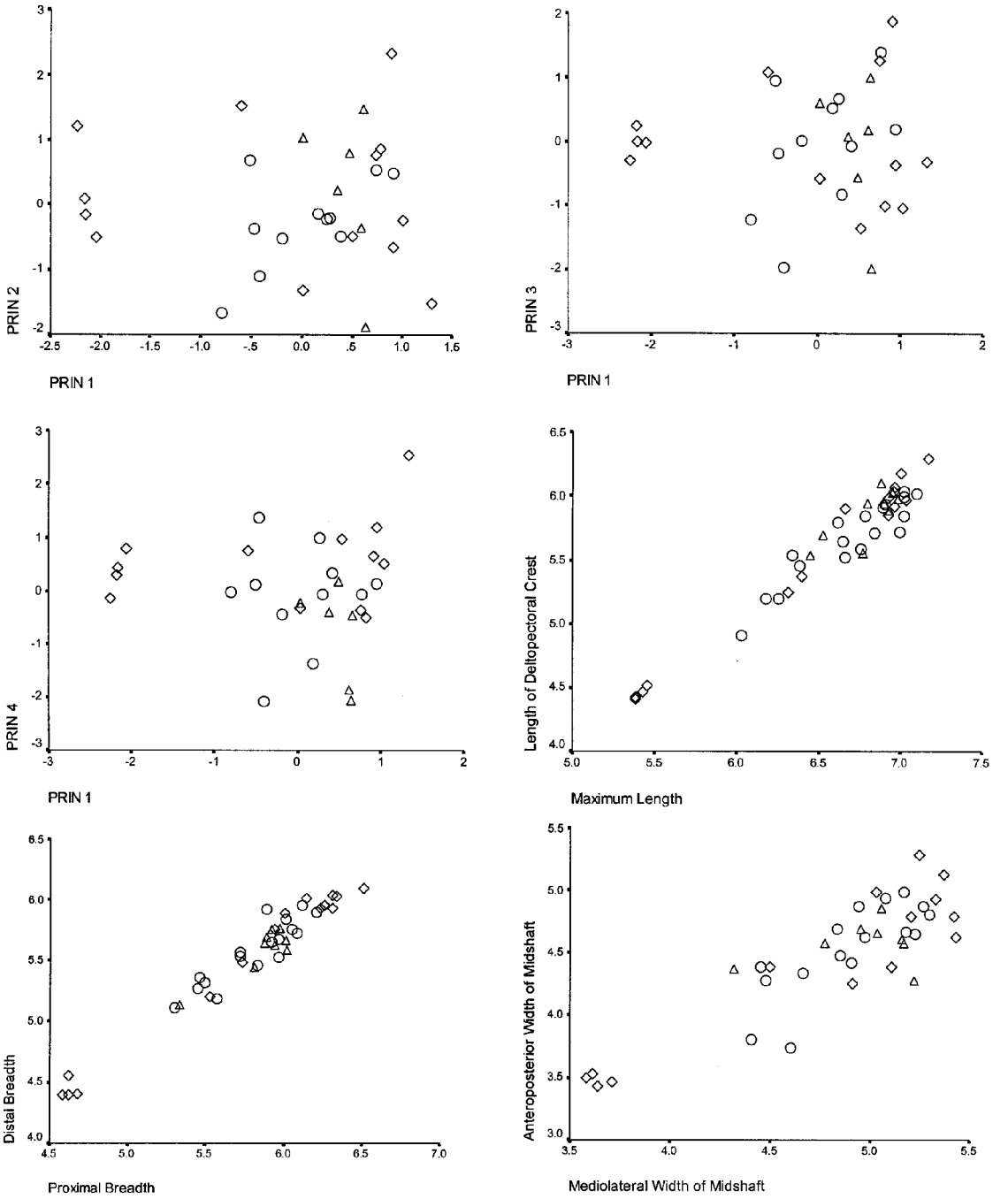

FIGURE 4. PCA and bivariate plots of humeri. All data are natural-log transformed. *Apatosaurus* is represented by diamonds, *Diplodocus* by triangles, and *Camarasaurus* by circles.

humerus length without affecting its overall isometric trend. Linear regression results show a great deal of individual variation for *Diplodocus* humeri. Several variables (anteroposterior midshaft width, condyle breadths, olecranon fossa dimensions) have low r^2 values and slopes that are not significantly different from zero (see Table 3). These variables show no discernible allometric or isometric trends for *Diplodocus*, but the very small sam-

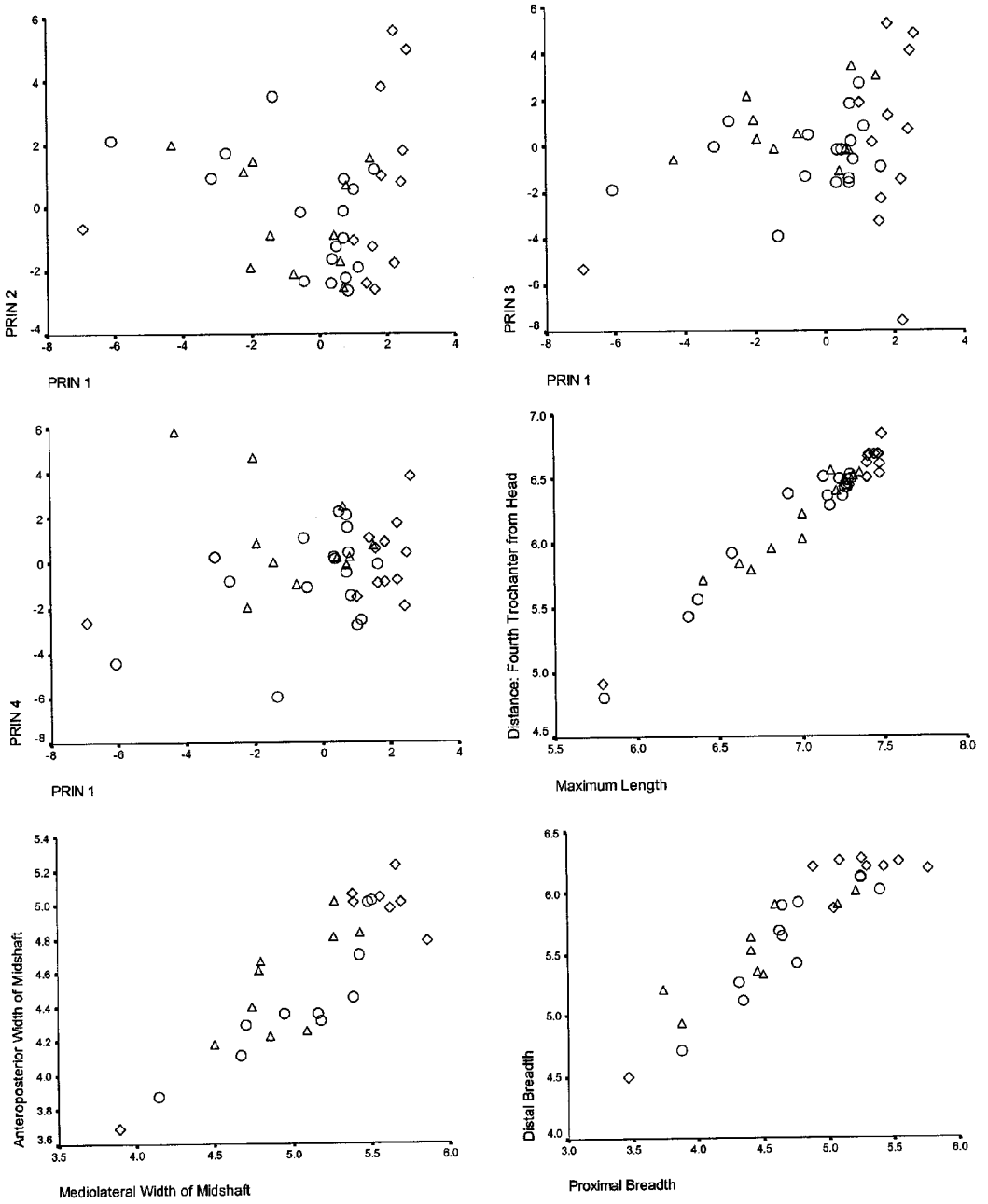

FIGURE 5. PCA and bivariate plots of femora. All data are natural-log transformed. See Figure 4 for legend.

ple size of *Diplodocus* humeri may have a substantial effect on these results. In the plot of mediolateral versus anteroposterior midshaft widths (H4, H5), *Diplodocus* humeri appear to expand more mediolaterally than anteroposteriorly as size increases, but it is unclear if this trend is a real biological signal or the result of a weak allometric trend for anteroposterior midshaft width. As with the PCA plots, the four *Apatosaurus* specimens that cluster at the left of each bivariate plot are juveniles.

Femur Results.—Data were generally absent for three variables in all genera, but especially in the diplodocids (*Apatosaurus*, *Diplodocus*):

TABLE 3. Results of linear regression of dependent variables against maximum humerus length in *Apatosaurus*, *Diplodocus*, and *Camarasaurus*. *p*-values are given for two null hypotheses tested with two-tailed *t*-tests ($\alpha = 0.05$): the slope is not significantly different from zero (H_0: $b_1 = 0$) and the slope is not significantly different from one (H_0: $b_1 = 1$). Nonsignificant differences are in boldface for H_0: $b_1 = 0$, whereas significant differences are in boldface for H_0: b_1 Variables defined in Table 2. Abbreviations: b_1, slope; r^2, adjusted r^2 value.

Variable	Taxon	r^2	df	SE	b_1	p H_0: $b_1 = 0$	p H_0: $b_1 = 1$
H2	All	0.928	38	0.046	0.9501	<0.05	>0.05
	Apatosaurus	0.980	13	0.043	1.0433	<0.05	>0.05
	Diplodocus	0.713	6	0.236	0.924	<0.05	>0.05
	Camarasaurus	0.867	15	0.082	0.7556	<0.05	**<0.05**
H3	All	0.957	39	0.037	0.9899	<0.05	>0.05
	Apatosaurus	0.984	13	0.036	1.0216	<0.05	>0.05
	Diplodocus	0.875	6	0.166	0.7638	<0.05	>0.05
	Camarasaurus	0.851	16	0.900	0.8702	<0.05	>0.05
H4	All	0.843	35	0.063	0.8781	<0.05	**<0.05**
	Apatosaurus	0.931	12	0.071	0.9284	<0.05	>0.05
	Diplodocus	0.263	5	0.347	0.4607	**>0.05**	>0.05
	Camarasaurus	0.722	14	0.150	0.9710	<0.05	>0.05
H5	All	0.937	38	0.042	1.0091	<0.05	>0.05
	Apatosaurus	0.971	13	0.052	1.0772	<0.05	>0.05
	Diplodocus	0.731	6	0.308	1.2509	<0.05	>0.05
	Camarasaurus	0.982	15	0.049	0.8420	<0.05	**<0.05**
H6	All	0.930	38	0.041	0.9026	<0.05	**<0.05**
	Apatosaurus	0.978	13	0.039	0.9877	<0.05	>0.05
	Diplodocus	0.743	6	0.211	0.9073	<0.05	>0.05
	Camarasaurus	0.911	15	0.065	0.7522	<0.05	**<0.05**
H7	All	0.807	36	0.087	0.8957	<0.05	>0.05
	Apatosaurus	0.914	13	0.085	1.0096	<0.05	>0.05
	Diplodocus	0.466	5	0.474	0.9774	**>0.05**	>0.05
	Camarasaurus	0.671	14	0.224	0.682	<0.05	>0.05
H8	All	0.926	36	0.042	0.9072	<0.05	**<0.05**
	Apatosaurus	0.967	13	0.053	0.9843	<0.05	>0.05
	Diplodocus	0.564	5	0.285	0.7277	**>0.05**	>0.05
	Camarasaurus	0.921	14	0.053	0.7805	<0.05	**<0.05**
H9	All	0.771	34	0.085	0.9388	<0.05	>0.05
	Apatosaurus	0.856	11	0.127	1.0295	<0.05	>0.05
	Diplodocus	0.038	5	0.552	0.7277	**>0.05**	**<0.05**
	Camarasaurus	0.850	14	0.082	0.7604	<0.05	**<0.05**
H10	All	0.895	30	0.059	0.9500	<0.05	>0.05
	Apatosaurus	0.947	11	0.070	0.9818	<0.05	>0.05
	Diplodocus	0.596	5	0.426	−0.2494	**>0.05**	>0.05
	Camarasaurus	0.826	10	0.089	0.6354	<0.05	**<0.05**

the crural extensor fossa breadth (F8), the crural extensor fossa height (F9), and the anteroposterior midshaft width (F12). Many of the diplodocid femora examined were stored, mounted, or damaged in such a way that measurement of their anterior surfaces was difficult or impossible. The missing data for the crural extensor fossa variables (F8, F9) alone would exclude 18 specimens from the PCA, severely truncating the large sample size and reducing the number of *Apatosaurus* ($n = 6$) and *Diplodocus* ($n = 6$) femora available for analysis. The truncation of diplodocid specimens over the three variables is worse, resulting in the retention of a single *Apatosaurus* femur for the PCA. Therefore, two PCAs were run. In the first PCA, the three problematic variables were deleted. In the second PCA, the missing values were estimated by substitution of means in the SPSS program (see Strauss et al. 2003: p. 289 for a recent review of this technique). Although this method is far from ideal because it tends to decrease variance and covariance estimates (Strauss et al. 2003), comparison of these results with those in the first PCA revealed no discernible differences, and both the PCA plots and their loadings were very similar. Therefore, to analyze and plot as many specimens as possible, the results of the second PCA were used and reported here. In

subsequent KW tests and bivariate plots of the femora, the patterns displayed in the PCA plots closely adhere to the patterns observed in the unmodified data.

Variable loadings suggest PC 2 is a contrast between greater trochanter breadth (F4) and the lateral condyle breadth (F10) and PC 3 is a contrast between crural extensor fossa height (F9) with medial condyle breadth (F11) and anteroposterior midshaft width (F12). PC 4 accounted for approximately 2% of the sample variation but retains small variable loadings that were difficult to interpret. All PCA plots show a distinct separation between *Apatosaurus* and the other two sauropod genera. All specimens plot in order of size along the PC 1 axis, and except for a single, juvenile outlier, all *Apatosaurus* specimens plot highly positively and extremely close to one another on PC 1, forming an almost linear and widely dispersed distribution along the other axes. Femora of *Diplodocus* and *Camarasaurus* are more widely distributed along PC 1 and the other components. All genera are widely distributed over PCs 2 and 3, making interpretation difficult. Because the crural extensor fossa height (F9) was largely a missing variable in *Apatosaurus* specimens, the wide scattering of this genus on PC 3 may also represent the bias of the statistical procedure used. However, the large scatter of *Diplodocus*, and especially of *Camarasaurus*, a genus that had the least amount of missing data, suggests that this pattern may reflect a real biological distribution.

KW tests showed a significant difference ($p < 0.05$) on all variables except medial condyle breadth (F11) and anteroposterior midshaft width (F12) (Table 4). Subsequent Mann-Whitney *U*-tests showed a statistically significant difference ($p < 0.0167$) on all remaining variables (except greater trochanter breadth [F4]) between *Apatosaurus* and the other two genera. Bivariate plots show the distinctive separation of *Apatosaurus* from *Diplodocus* and *Camarasaurus* and show clearly that *Apatosaurus* femora are massive bones. Most *Apatosaurus* specimens cluster together near the larger end of the axes, and in the plots of midshaft width and proximal/distal breadth this clustering is taken to an extreme. In particular, the plot of proximal versus distal breadth is of note: with two exceptions, the distal breadth measurement value for most *Apatosaurus* femora remains essentially constant with increasing size, whereas proximal breadth values change appreciably.

TABLE 4. Results of Kruskal-Wallis and Mann-Whitney *U*-tests for the femur. Numbers represent *p*-values. $\alpha = 0.05$ for Kruskal-Wallis tests; $\alpha = 0.0167$ for Mann-Whitney *U*-tests. Abbreviations: KW, Kruskal-Wallis test; *U*, Mann-Whitney *U*; C/A, *Camarasaurus* vs. *Apatosaurus*; C/D, *Camarasaurus* vs. *Diplodocus*; A/D, *Apatosaurus* vs. *Diplodocus*. Variables defined in Appendix 2.

Variable	KW test	*U*-test C/A	*U*-test C/D	*U*-test A/D
F1	0.000	0.000	0.906	0.001
F2	0.001	0.001	0.657	0.002
F3	0.001	0.002	0.459	0.002
F4	0.041	0.072	0.324	0.017
F5	0.001	0.001	0.863	0.005
F6	0.004	0.008	0.199	0.004
F7	0.001	0.002	0.095	0.003
F8	0.009	0.012	0.191	0.009
F9	0.001	0.002	0.459	0.001
F10	0.011	0.020	0.171	0.011
F11	0.066			
F12	0.055			
F13	0.003	0.010	0.086	0.003

The slope equations on the measurement variables show some allometric trends among the genera (Table 5). As with the humerus, many variables plot nearly isometrically against maximum length. *Apatosaurus* shows some positively allometric trends (femoral head breadth, fourth trochanter distance, crural extensor fossa dimensions) that probably correlate with the overall robustness of this taxon's femur. For *Camarasaurus*, negative allometric slopes are reported for most mediolateral dimensions of the femur (see Table 5). These results correlate with similar trends in the humerus (see above) and again suggest that mediolateral expansion of the femur lagged slightly behind overall femur size increases. All taxa show lower moderately negative allometric slopes for the anteroposterior than mediolateral midshaft width (which are isometric [*Apatosaurus*, *Diplodocus*] or negative [*Camarasaurus*]), suggesting that this feature of their femora expands at a slower rate as size increases (see Table 5). This result would correlate with the typically oval cross-section of sauropod femora. *Diplodocus* shows positive

TABLE 5. Results of linear regression of dependent variables against maximum femur length in *Apatosaurus*, *Diplodocus*, and *Camarasaurus*. See Table 3 for more information. Variables defined in Appendix 2.

Variable	Taxon	r^2	df	SE	b_1	p H_0: $b_1 = 0$	p H_0: $b_1 = 1$
F2	All	0.935	36	0.042	0.9635	<0.05	>0.05
	Apatosaurus	0.982	9	0.045	1.0257	<0.05	>0.05
	Diplodocus	0.958	9	0.107	1.2343	<0.05	**<0.05**
	Camarasaurus	0.932	14	0.057	0.8578	<0.05	**<0.05**
F3	All	0.933	36	0.055	1.0412	<0.05	>0.05
	Apatosaurus	0.943	9	0.089	1.2304	<0.05	**<0.05**
	Diplodocus	0.953	9	0.133	1.0884	<0.05	>0.05
	Camarasaurus	0.908	14	0.073	0.9210	<0.05	>0.05
F4	All	0.717	36	0.088	0.831	<0.05	>0.05
	Apatosaurus	0.697	9	0.176	0.5971	<0.05	**<0.05**
	Diplodocus	0.815	9	0.221	1.563	<0.05	**<0.05**
	Camarasaurus	0.827	14	0.109	0.7697	<0.05	>0.05
F5	All	0.964	37	0.035	1.1055	<0.05	**<0.05**
	Apatosaurus	0.973	10	0.052	1.136	<0.05	**<0.05**
	Diplodocus	0.933	9	0.098	1.039	<0.05	>0.05
	Camarasaurus	0.950	14	0.063	1.1087	<0.05	>0.05
F6	All	0.886	36	0.067	0.9706	<0.05	>0.05
	Apatosaurus	0.872	9	0.130	1.0792	<0.05	>0.05
	Diplodocus	0.797	9	0.149	1.0169	<0.05	>0.05
	Camarasaurus	0.869	14	0.095	0.9190	<0.05	>0.05
F7	All	0.948	37	0.048	0.9221	<0.05	**<0.05**
	Apatosaurus	0.969	9	0.058	0.9956	<0.05	**<0.05**
	Diplodocus	0.980	9	0.113	1.1284	<0.05	>0.05
	Camarasaurus	0.944	15	0.053	0.8314	<0.05	**<0.05**
F8	All	0.767	28	0.119	0.9400	<0.05	>0.05
	Apatosaurus	0.870	8	0.146	1.3579	<0.05	**<0.05**
	Diplodocus	0.825	7	0.401	1.2686	<0.05	>0.05
	Camarasaurus	0.728	9	0.149	0.6166	<0.05	**<0.05**
F9	All	0.756	20	0.098	0.8535	<0.05	>0.05
	Apatosaurus	0.952	4	0.120	1.3154	<0.05	**<0.05**
	Diplodocus	0.927	4	0.141	1.0036	<0.05	>0.05
	Camarasaurus	0.642	8	0.127	0.4829	<0.05	**<0.05**
F10	All	0.789	33	0.077	0.8532	<0.05	**<0.05**
	Apatosaurus	0.907	8	0.112	1.0181	<0.05	**<0.05**
	Diplodocus	0.847	8	0.180	1.1716	<0.05	>0.05
	Camarasaurus	0.692	13	0.110	0.6708	<0.05	**<0.05**
F11	All	0.736	37	0.103	0.8724	<0.05	**<0.05**
	Apatosaurus	0.748	10	0.184	0.8974	<0.05	**<0.05**
	Diplodocus	0.944	9	0.128	1.1145	<0.05	>0.05
	Camarasaurus	0.606	14	0.166	0.8083	<0.05	**<0.05**
F12	All	0.721	25	0.084	0.6627	<0.05	>0.05
	Apatosaurus	0.913	6	0.093	0.7784	<0.05	>0.05
	Diplodocus	0.541	7	0.274	0.6938	<0.05	>0.05
	Camarasaurus	0.619	8	0.151	0.5679	<0.05	**<0.05**
F13	All	0.946	36	0.052	0.9278	<0.05	>0.05
	Apatosaurus	0.934	8	0.092	1.0612	<0.05	>0.05
	Diplodocus	0.998	9	0.090	1.0044	<0.05	>0.05
	Camarasaurus	0.950	15	0.060	0.8386	<0.05	>0.05

allometric trends on the variables of proximal breadth and greater trochanter breadth.

Thin-plate Splines

Humerus Results.—Twenty-nine of the 41 humeri specimens were suitable for photography and digitizing (*Apatosaurus* [$n = 9$]; *Diplodocus* [$n = 6$]; *Camarasaurus* [$n = 14$]). MANOVA results indicate that there is a significant multivariate difference in humerus shape among the genera on both the uniform components and partial warps, and between-subjects tests show the significant variables to be Uniform Y, Y1, and X8 (Table 6). Post hoc pairwise comparisons (with Bonferroni corrections) report a significant difference between

TABLE 6. MANOVA results for the uniform components and partial warps of the humerus. Uniform components and partial warps were tested separately. $\alpha = 0.05$ for all tests. *, multivariate significance for Pillai's Trace, Wilk's Lambda, Hotelling's Trace, and Roy's Largest Root; †, post hoc Bonferroni significance between *Apatosaurus* and other taxa; ‡, post hoc Bonferroni significance between *Apatosaurus* and *Diplodocus*.

Component	Test	*F*	*p*	Component	Test	*F*	*p*
Total uniform	Multivariate	*	*	Total partial warps	Multivariate	*	*
Uniform X	Between-subjects	0.513	0.605	Uniform Y	Between-subjects	21.776	0.000†
X1		1.797	0.186	Y1		4.325	0.024‡
X2		0.081	0.922	Y2		0.172	0.843
X3		1.703	0.202	Y3		0.319	0.730
X4		2.592	0.094	Y4		3.284	0.053
X5		2.726	0.084	Y5		2.080	0.145
X6		1.869	0.174	Y6		1.001	0.381
X7		1.724	0.198	Y7		1.037	0.369
X8		6.779	0.004†	Y8		2.960	0.069

Apatosaurus and the other two genera on Uniform Y and X8, and between *Apatosaurus* and *Diplodocus* on Y1 (Table 6). The plot of uniform components (Fig. 6) shows a clear separation of *Apatosaurus* from *Diplodocus* and *Camarasaurus* on the Uniform Y axis. Uniform Y represents a morphometric continuum of mediolateral humerus expansion: along its positive axis landmarks move farther apart from one another, whereas landmarks move toward each other along its negative axis. Most *Apatosaurus* humeri fall along the positive range of Uniform Y, in contrast to most *Camarasaurus* and all *Diplodocus* humeri that plot negatively. Uniform X represents a continuum of lateral (negative) to medial (positive) humerus shear, but an approximately equal number of specimens are distributed across its axis. In the plot of X8-Y8 (Fig. 6), *Apatosaurus* specimens are clearly separate from most *Diplodocus* and *Camarasaurus* humeri on Y8, a component of proximal humerus elongation. Along the positive axis, the deltopectoral crest (5) and midshaft (6, 11) landmarks shift distally, elongating the proximal end of the humerus, extending the deltopectoral crest, and displacing the midshaft constriction from the center of the shaft. In contrast, the same landmarks are shifted proximally along the negative axis of Y8, truncating the proximal end of the humerus and displacing the midshaft constriction toward the humeral head. X8 is a component of medial (negative) to lateral (positive) humerus ''bending,'' but no distinct separation of genera is apparent along its axis. The plot of X1-Y1 (Fig. 6) details small-scale changes in humerus shape associated with the distal ridges (landmarks 8 and 9). The significant difference reported for *Apatosaurus* and *Diplodocus* along the Y1 axis is not clear from the plot, but is apparently associated with a small shift in the distance between the distal ridges. No other distinct patterns are visible.

The first four relative warps (RWs) account for over 80% of the total sample shape variation (Table 8) and RW 1 describes most of the shape variation present in the humeri. According to the MANOVA of the partial warps, the humerus of *Apatosaurus* is significantly different from those of *Diplodocus* and *Camarasaurus* in being expanded mediolaterally and elongated proximally with a distally displaced deltopectoral crest and midshaft constriction. These differences are summarized in the plot of RW 1 versus RW 2 (Fig. 6). All *Apatosaurus* specimens except one plot negatively on RW 1 and occupy the two left quadrants. *Diplodocus* and *Camarasaurus* overlap one another, and most occupy much of the same morphospace along the positive aspect of the RW 1 axis in the two right quadrants. RW 1 represents a morphometric continuum of humerus robustness and expansion: as RW 1 becomes negative, the landmarks corresponding to the proximal (1–4) and distal (7–10) ends of the humerus expand, the deltopectoral crest (5) and midshaft constriction (6, 11) shift distally, and the medial ''epicondyle'' of the humerus (9, 10) expands. As RW 1 becomes positive, humeri become narrow and

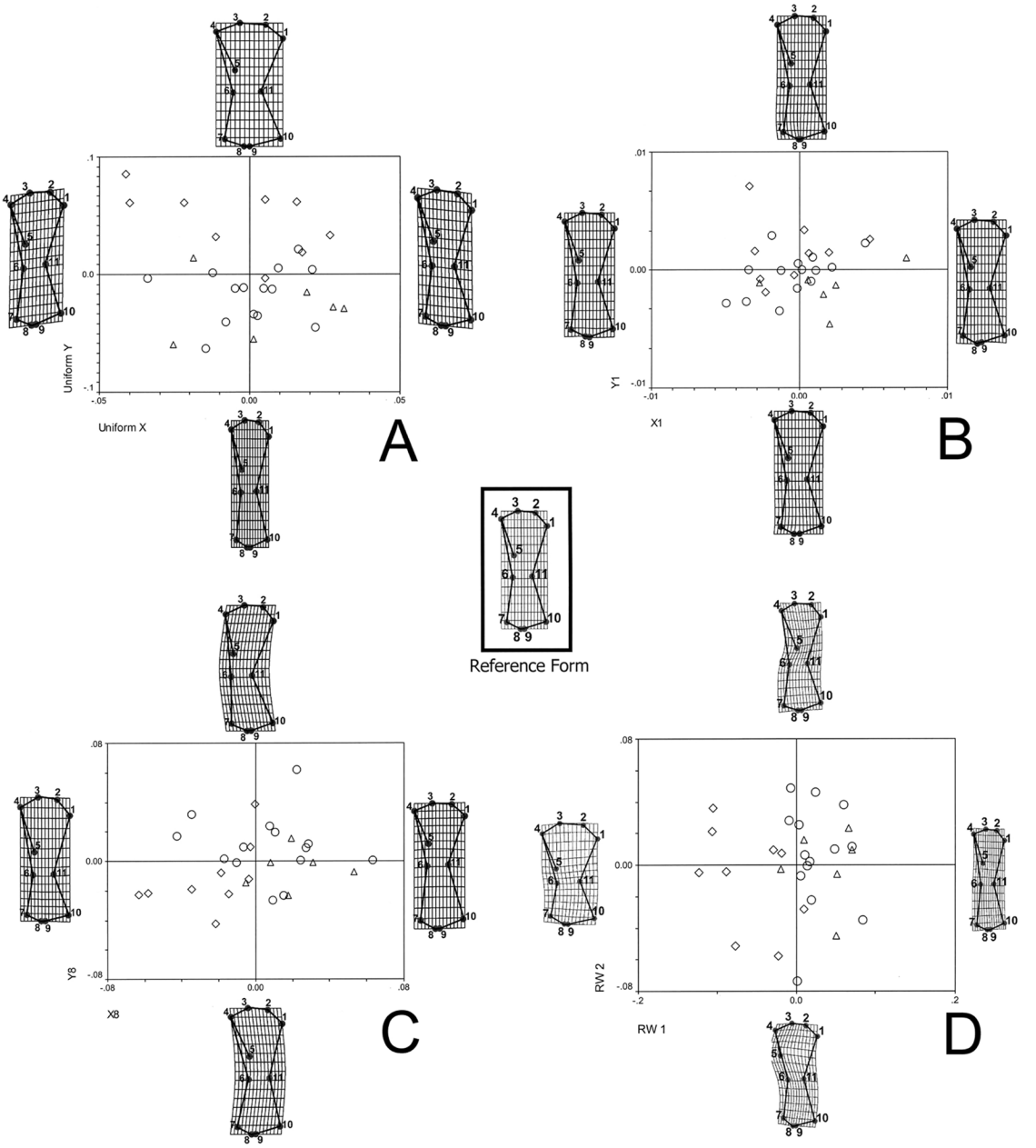

FIGURE 6. Thin-plate splines plot of partial and relative warp scores for humeri. A, Uniform components; B, X1 vs. Y1; C, X8 vs. Y8; D, Relative warps. See Figure 4 for legend.

elongate, and the deltopectoral crest and mid-shaft constriction shift proximally. RW 2 is a shape variable affected mostly by the position of the deltopectoral crest: as RW 2 becomes negative, the deltopectoral crest landmark (5) shifts laterally, and medially as RW 2 becomes positive.

The landmarks corresponding to the medial ''epicondyle'' (9, 10) become more expanded in *Apatosaurus*, and the lateral ''epicondyle'' landmarks (7, 8) have moved closer together. The two juvenile *Apatosaurus* humeri (CM 566 and OMNH 01277) plot close to the reference form (the origin of the plot). The relatively constrained positive range of most *Diplodocus* and *Camarasaurus* humeri on RW 1 places

TABLE 7. MANOVA results for the uniform components and partial warps of the femur. Uniform components and partial warps were tested separately. $\alpha = 0.05$ for all tests. *, multivariate significance for Pillai's Trace, Wilk's Lambda, Hotelling's Trace, and Roy's Largest Root; ns, no significant multivariate difference; †, post hoc Bonferroni significance between *Diplodocus* and other taxa.

Component	Test	*F*	*p*	Component	Test	*F*	*p*
Total uniform	Multivariate	*	*	Total partial warps	Multivariate	ns	ns
Uniform X	Between-subjects	1.433	0.272	Uniform Y	Between-subjects	12.989	0.001†
X1		0.303	0.743	Y1		1.069	0.370
X2		0.603	0.561	Y2		0.636	0.544
X3		0.496	0.619	Y3		1.494	0.258
X4		0.983	0.399	Y4		2.204	0.147
X5		1.665	0.225	Y5		1.224	0.324
X6		0.361	0.703	Y6		3.249	0.069

them in a morphospace where the landmarks of the proximal and distal ends (1–4, 7–10) of the humerus have moved closer together and stretched apart lengthwise. Furthermore, the deltopectoral crest (5) and midshaft constriction (6, 11) have shifted proximally. All humeri are distributed broadly across the RW 2 axis, and this shows that the relative position of the deltopectoral crest (landmark 5) varies randomly among the genera and suggests its relative position may not result from biological processes. Analysis of RW 3 and RW 4 showed similar but less distinct patterns of deltopectoral crest position, again with no distinct groupings of the genera. The significant difference reported between *Apatosaurus* and *Diplodocus* on the localized distal ridge placement (Y1) was not reflected in the relative warps analysis. Overall, RW 1 best summarizes the suite of significant morphological changes reported for the uniform components and partial warps (see above).

Femur Results.—Only 17 of the 40 sauropod femora were available for relative warps analysis. This is because the femora of well-preserved, large sauropods tend to be placed in skeletal mounts or displayed in such a way that controlled photography or photography of the appropriate face of the femur was impossible. Whereas several specimens of *Camarasaurus* ($n = 6$) and *Diplodocus* ($n = 7$) were available for photography, eight of the 12 *Apatosaurus* femora either were placed in skeletal mounts or were otherwise inaccessible. MANOVA results indicate that there was no significant multivariate effect on the partial warps, but there was a significant difference among the genera on the uniform components (Table 7). *Diplodocus* is shown to be significantly different from *Apatosaurus* and *Camarasaurus* on the Uniform Y component (Table 7). As with the humerus, Uniform Y is a component of femoral expansion: landmarks move apart from one another mediolaterally along its positive axis, with the reverse trend along the negative axis. Uniform X is a component of medial (negative) and lateral (positive) femoral shear. All *Diplodocus* femora plot along the negative axis of Uniform Y, and most plot in the lower left quadrant, showing trends toward a gracile form and medial femoral shear. Most *Apatosaurus* and *Camarasaurus* femora plot along the positive axis of Uniform Y, correlating with a more mediolaterally expanded femur, but are widely distributed across Uniform X.

The first four extracted RWs account for 86% of the total sample variation and, as with the humerus, RW 1 describes most of the shape variation in the sample (Table 8). RW 1 represents a morphometric continuum of femoral robustness and the position of the fourth trochanter (Fig. 7). The more negatively a specimen plots along the RW 1 axis, the more expanded the proximal and distal ends become (landmarks 1–3, 6, 7) while the fourth trochanter (landmark 4) and lesser trochanter (landmark 9) move farther distally from the femoral head. The more positively a specimen plots on RW 1, the more gracile and slender is the femoral shaft, and the more proximally located the fourth and lesser trochanters are to the femoral head. Changes in the position of the fourth and lesser trochanters are surpris-

TABLE 8. Relative warps results for the humerus and femur. The first ten relative warps are listed; they account for 99.08% and 99.53% of the total sample variation for the humerus and femur, respectively. Relative warps were not weighted ($\alpha = 0$) and the uniform component was included in the analysis (see TPSRW documentation [Rohlf 1997b]). Singular values are eigenvalues of traditional PCA. Abbreviations: RW, relative warp.

RW Humerus	Singular values	% Variance	RW Femur	Singular values	% Variance
1	0.29696	48.02	1	0.18905	39.44
2	0.16297	14.46	2	0.13528	20.19
3	0.14012	10.69	3	0.12293	16.68
4	0.12522	8.54	4	0.09481	9.92
5	0.10035	5.48	5	0.06482	4.64
6	0.08574	4.00	6	0.05111	2.88
7	0.06797	2.52	7	0.04483	2.22
8	0.05530	1.67	8	0.03761	1.56
9	0.04876	1.29	9	0.03451	1.31
10	0.04528	1.12	10	0.02503	0.69

ing because these changes are not apparent in the morphometric or partial warps analyses. RW 2 reflects a morphological continuum in which the position of the constriction of the midshaft and the size of the greater trochanter changes. The more positively a specimen plots along the axis of RW 2, the more expanded the greater trochanter region (landmarks 1, 2) becomes, and the more proximally its midshaft constriction (landmarks 5, 8) is to the femoral head. Negatively plotting specimens show a reversed trend.

All *Camarasaurus* specimens and three of the four *Apatosaurus* specimens plot negatively along the RW 1 axis, whereas all *Diplodocus* specimens and the juvenile *Apatosaurus excelsus* (CM 566) specimen plot positively. This plot reveals three distinctive morphological trends not observed in the PCA, linear regressions, or partial warps. First, both *Camarasaurus* and the adult *Apatosaurus* femora, in addition to being more robust than *Diplodocus*, show distinctly wider femoral heads and greater trochanters. Second, the positions of the fourth and lesser trochanters are more distally located in *Camarasaurus* and in the adult *Apatosaurus* specimens than in *Diplodocus*. Third, the juvenile *Apatosaurus* femur plots with the adult *Diplodocus* specimens, and this juvenile specimen has a gracile shape with a more proximally placed fourth trochanter. The wide distribution of all three genera along the RW 2 axis suggests that the relative size of the greater trochanter and the position of midshaft constriction result from individual var-

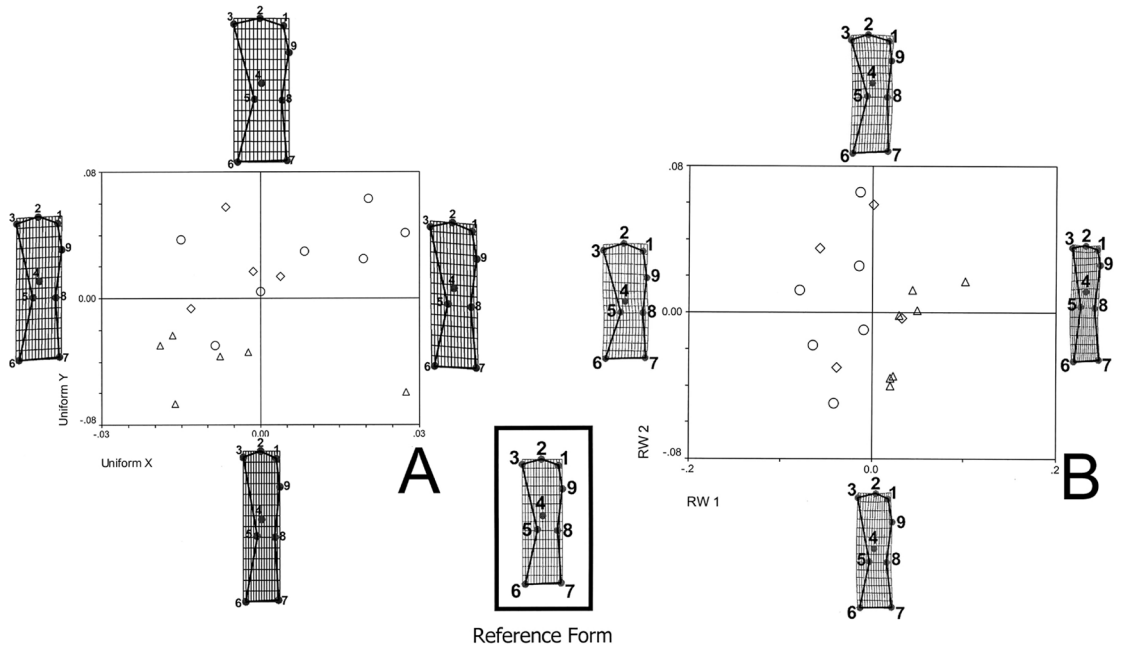

FIGURE 7. Thin-plate splines plot of partial and relative warp scores for femora. A, Uniform components; B, Relative warps. See Figure 4 for legend.

iation. This supports the suggestion raised earlier with PCA that individual variation, and perhaps factors such as diagenesis, caused the wide distribution of specimens along the PC 2 axis where width of the greater trochanter was a contributing variable. RWs 3 and 4 are components of femoral ''bending'' but showed no distinct partitioning of the genera. Overall, RW 1 summarizes the significant morphological changes reported for the uniform components, but also shows variation in the position of the lesser and fourth trochanter landmarks.

Discussion

Functional Morphology

Humerus.—Morphometric patterns for humeri based on linear measurement data are, with few exceptions, size related. Given the large size discrepancies between the smallest and largest individuals in the sample, it is perhaps not surprising that significant differences were not detected on any variable for any taxon. Such results on sets of fewer variables have been reported previously for sauropod humeri (Foster 1995; Curtice et al. 1997; Wilhite and Curtice 1998; Wilhite 1999), and the correlation of these data with results presented here bolsters a suggestion advocated by Wilhite and Curtice (1998) and Wilhite (1999) that appendicular ontogeny in sauropods was isometric. Such a growth trajectory is uncommon or unreported among terrestrial vertebrates and merits closer examination. The biological implications of isometric growth in sauropods will be addressed in more detail elsewhere (Bonnan unpublished data). For the present study, a few observations are worth noting. The isometric pattern may simply be the result of poor resolution of linear morphometric patterns, and without appropriate shape-based morphometric data or comparison with other taxa, such a hypothesis is difficult to test. Furthermore, as with many sauropsids (Haines 1942) and dinosaurs (Horner et al. 2001), the exact morphology of the epiphysis is not preserved in sauropod limbs (McIntosh 1990) because it was not secondarily ossified. Thus, an isometric slope may simply reflect the overall growth of the diaphysis. However, some evidence that the observed isometry is a ''real'' biological signal in sauropods, and not simply a result of gross size differences, is provided by the relative warps analysis. Surprisingly, although it elucidated shape differences among the three genera, the relative warps analysis produced no clear distinction in shape between smaller and larger individuals within a taxon (see below). Overall, traditional morphometric analyses provided little resolution of shape differences among humeri of the three genera.

Partial and relative warps results show that significant shape differences are present among the sauropod humeri examined here. Overall, the results show that the humeri of *Apatosaurus* are typically wider and more robust than those of *Diplodocus* and *Camarasaurus*. This observation is not surprising and has often been used to differentiate between *Apatosaurus* humeri and those of other sauropods (McIntosh 1990). However, unlike a PCA or linear regression, the partial and relative warps results show where the expansion and shape change in the humerus occur specifically. The proximal expansion of the humerus in *Apatosaurus* extends the region of the humeral head (landmarks 2 and 3) and the medial and lateral portions of the proximal humerus as well. The landmarks 3 and 4 define a proximal region that accommodates the insertion of the M. supracoracoideus in lepidosaurs and crocodilians (Reese 1915; Romer 1956; Bonnan 2001). This muscle augments the actions of the pectoralis, namely flexion, medial rotation, and adduction of the humerus (Romer 1956). In birds, the function of M. supracoracoideus has been modified to abduct the humerus and lift the wing. It inserts posteriorly instead of anteriorly in this region because its tendon has been reoriented through a triosseal canal (Proctor and Lynch 1993). The quadrupedal stance of sauropods suggests M. supracoracoideus inserted anteriorly rather than posteriorly in the region of landmarks 3 and 4. The posterior face of the region medial to the humeral head, defined by landmarks 1 and 2, is the region in which the large rotator cuff muscle, M. subcoracoscapularis, inserts on the humerus in lepidosaurs, crocodilians (Reese 1915; Romer 1956; Bonnan 2001), and

birds (Romer 1962; Proctor and Lynch 1993). This muscle both stabilizes the humerus and keeps its head articulated with the scapulocoracoid glenoid. Although this muscle inserts posterior to the region of landmarks 1 and 2, this region is flattened anteroposteriorly in sauropods. Therefore, the posterior side of this region is approximately equal in area to the anterior side. The expansion of the proximal region (landmarks 1–4) in *Apatosaurus* suggests the M. supracoracoideus and M. subcoracoscapularis insertions in these regions were also expanded. As *Apatosaurus* is the most robust of the three genera examined here, such enlarged regions for muscle attachment may simply be correlated with its more massive skeletal frame.

The more elongate deltopectoral crest of *Apatosaurus* suggests that the scapular deltoids, M. pectoralis, M. latissimus dorsi, and musculature homologous to the major deltopectoral groups of lepidosaurs (Romer 1956), crocodilians (Reese 1915; Romer 1956; Bonnan 2001), and birds (Proctor and Lynch 1993) expanded their gross size, tendinous insertion, or both in this taxon. As with the proximal expansion of the humerus, elongation of the deltopectoral crest in *Apatosaurus* may simply be correlated with its more massive skeleton. One of the most striking features of the humerus of *Apatosaurus* illustrated by thin-plate splines is the greatly expanded medial border of its distal end (for simplicity referred to as the medial ''epicondyle''). In lepidosaurs, crocodilians, and birds the medial border or epicondyle of the humerus is the origin for the major flexors of the manus and carpus (Reese 1915; Romer 1956, 1962; Proctor and Lynch 1993; Hildebrand and Goslow 2001). By outgroup comparison, this suggests that the distal expansion of the medial ''epicondyle'' in *Apatosaurus* provided an expanded site of origin for manus and carpus flexors. Medial ''epicondyle'' expansion in this genus may be correlated with manus morphology. It is noteworthy that the manus of *Apatosaurus* is short and robust and retains a very large pollex claw (Upchurch 1994; Bonnan 2001, 2003) in contrast to many other sauropods. For example, *Camarasaurus* has an elongate metacarpus and gracile pollex claw, whereas *Diplodocus* has a short but gracile manus and pollex claw (Bonnan 2001). Flexion of a robust manus and pollex claw in *Apatosaurus* may have required the development of large manus flexor musculature, which would be correlated with an expanded medial ''epicondyle.''

In *Diplodocus* and *Camarasaurus*, the proximal and distal ends of the humerus are equally expanded, and both genera exhibit a trend toward slenderness in the humerus. Such a trend is surprising both because it is unapparent in the linear morphometric data and because it would not be predicted from casual inspection of *Camarasaurus* humeri. Many *Camarasaurus* individuals are quite large (e.g., *C. supremus*) and their humeri appear more robust than those of *Diplodocus* specimens of similar size during qualitative visual inspection. The results of the partial and relative warps suggest, however, that the humerus of *Camarasaurus* is much more slender than that of *Apatosaurus* and has less-expanded regions for inferred muscular insertion (e.g., M. supracoracoideus and M. subcoracoscapularis) than might be expected. Overall, the humeri of *Diplodocus* and *Camarasaurus* are typically less robust and more elongate than those of *Apatosaurus*, and the deltopectoral crest is less elongate, terminating more proximally in many specimens. More-proximal insertions of deltopectoral muscles over a smaller area in these genera suggest there were differences in the lever advantage and power of these muscles among *Apatosaurus*, *Diplodocus*, and *Camarasaurus*.

Assuming a columnar orientation for the humerus and limited long-axis rotation, the results from the thin-plate splines indicate the following regarding functional morphology: For all three taxa, deltopectoral muscles would act mostly to draw the humerus anteriorly in flexion. The action of the deltopectoral muscles on the humerus corresponds to the in-force of a second-order lever system, where the humeral head would function as the fulcrum and the humerus shaft would constitute the out-lever (see Hildebrand and Goslow 2001 and Liem et al. 2001 for a summary and examples of biological lever systems). In such a system, both the in-force and out-force are applied on the same side of the fulcrum. The

more distally from the fulcrum (humeral head) the in-force (deltopectoral muscle action) is applied, the greater the turning moment or torque of the out-lever (humerus shaft) about the fulcrum becomes (see Hildebrand and Goslow 2001 and Liem et al. 2001). Simultaneously, the more distally placed the in-force is from the fulcrum, the smaller the arc of out-lever rotation about the fulcrum. In *Apatosaurus*, the more elongate deltopectoral crest suggests that the insertion sites of the deltopectoral muscles would be located farther from its humeral head. This would act to increase the force with which these muscles acted upon the humerus while decreasing its arc of flexion. In contrast, the shorter, more proximally terminating deltopectoral crest of *Diplodocus* and *Camarasaurus* would situate the deltopectoral in-force more proximally to the humeral head. This would result in a lower turning moment of the humerus about the glenoid, but allow it to flex through a longer arc than would be predicted for *Apatosaurus*.

In all three taxa, the regions between landmarks 1–2 and 3–4 correspond to the probable insertion sites of M. subcoracoscapularis and M. supracoracoideus, respectively, according to EPB analysis. As M. supracoracoideus probably functioned to augment humerus flexion, the corresponding expansion of the landmark 3–4 region in *Apatosaurus* correlates well with the inferred large in-force for the deltopectoral muscles in this taxon. The narrower landmark 3–4 region in *Diplodocus* and *Camarasaurus* suggests an opposite trend based on their inferred deltopectoral in-force. In other words, the area of the inferred M. supracoracoideus insertion site becomes more expanded as the inferred degree of deltopectoral in-force increases. The M. subcoracoscapularis probably facilitated stabilization of the humeral head within the scapulocoracoid glenoid as it does in the outgroup taxa. Again, the expansion of the landmark 1–2 region would correlate with the greater deltopectoral in-force inferred for *Apatosaurus*, whereas the narrowing of this region coincides with the smaller deltopectoral in-force inferred for *Diplodocus* and *Camarasaurus*.

Femur.—As with the humerus, PCA and bivariate plots typically show isometric, size-related trends. However, more allometric trends were reported for the femur than for the humerus. Most of the data suggest that *Apatosaurus* had more robust and massive femora than *Diplodocus* or *Camarasaurus*. Again, this result was expected and has been reported as a defining characteristic of *Apatosaurus* (e.g., McIntosh 1990). One curious outcome apparent in the PCA and bivariate plots was the tight clustering of *Apatosaurus* femora at the high end of the size range without the broader spread observed for *Diplodocus* and *Camarasaurus*. From a functional perspective, the conspicuously narrow range of *Apatosaurus* femora in the PCA and bivariate plots may reflect a growth strategy. Histological analysis of scapulae, radii, and ulnae by Curry (1999) suggests that *Apatosaurus* grew rapidly. One possibility is that *Apatosaurus* grew to large size more rapidly than the other two genera, and therefore the available fossil sample of small to mid-sized *Apatosaurus* specimens is relatively small. Without comparative histological data from *Diplodocus* and *Camarasaurus*, however, this suggestion is difficult to corroborate. Furthermore, it would not explain the more typical distribution of *Apatosaurus* humeri discussed above. *Diplodocus* femora show positive allometry for proximal and greater trochanter breadth, results that suggest the proximal end of the femur expanded at a faster rate in this gracile taxon than in *Camarasaurus* or *Apatosaurus*. As reported above, mediolateral midshaft breadth increased faster with size than did anteroposterior width in all the genera, and this trend appears to correspond with the typically oval shape of the femur in cross-section. Because the sauropod femur was loaded off-center, it has been suggested that an anteroposteriorly flattened femoral cross-section would reduce the radial shear produced under such stress (Wilson and Sereno 1998).

The results from the partial and relative warps greatly clarified the morphological differences among the genera, especially between *Diplodocus* and *Camarasaurus*. Differences in the position of the fourth trochanter (landmark 4), as revealed by the relative warps, were especially surprising because they were not detected with any of the tradi-

tional morphometric techniques. The fourth trochanter is associated with M. caudofemoralis longus and M. caudofemoralis brevis in lepidosaurs and crocodilians, muscles that function as powerful femoral retractors (Romer 1956, 1962; Gatesy 1990, 1995, 1997). The M. caudofemorales have been reduced in birds (Gatesy 1995, 1999; Gatesy and Middleton 1997). It is well-established that the fourth trochanter is associated with the M. caudofemorales in dinosaurs (e.g., Gatesy 1990, 1995), so differences in fourth trochanter location on the femoral shaft in sauropods are inferred to correlate with differences in caudofemoral muscle insertion. The more proximal location of the fourth trochanter in *Diplodocus*, and its more distal location in most *Apatosaurus* and *Camarasaurus* specimens, suggests there were differences in the mechanical advantage of the M. caudofemorales among the taxa (see below).

The area between landmarks 1 and 2 corresponds to a region typically referred to as the greater trochanter in dinosaurs (see Walker 1977 for an overview). In lepidosaurs and crocodilians, the dorsal branch of M. puboischiofemoralis internus (PIFI) usually inserts just anterior to this region (e.g., Romer 1923a,b, 1956, 1962; Walker 1977) where it effects some femoral protraction (Walker 1977). The PIFI is extremely reduced in birds, with the retention of a single, medial head commonly named M. iliacus (Walker 1977). The so-called greater trochanter of dinosaurs is generally continuous with the articular surface of the femoral head and not well-defined. This landmark's variability among dinosaurs and its close resemblance to an articular surface suggests it is either a continuation of the femoral head or an attachment site for a bursa over which other femoral protractors (e.g., M. iliofemoralis and M. iliofibularis) passed (Walker 1977). If PIFI inserted anterior to this region in dinosaur femora and functioned as a protractor (as per Walker 1977), then perhaps the expanse of region 1–2 in the sauropod femora correlates with the general size of this muscle. However, as this muscle is inferred to have inserted posterior to region 1–2, its soft tissue associations are unclear, and because its ''size'' is apparently correlated simply with femur robustness (see Fig. 7), no functional inferences will be drawn from this region.

Landmark 9 is associated with a lateral bulge on the femur that is typically interpreted as the lesser trochanter in dinosaurs (Romer 1956; Walker 1977). This lateral region in lepidosaurs and crocodilians is the insertion site for M. iliofemoralis, a muscle that effects some femoral abduction and holds the femoral head against the acetabulum (Romer 1956, 1962; Walker 1977). In birds, M. iliofemoralis appears to have been modified into several M. iliotrochanterici that insert into an anterior trochanteric ridge (probably homologous to the dinosaur lesser trochanter) and function mostly to stabilize and protract the femur (George and Berger 1966; Walker 1977; Proctor and Lynch 1993; Gatesy 1999). In theropods, the lesser trochanter is located on the anterolateral side of the femur approximately one-third the length of the shaft distally from the femoral head, whereas this landmark is more reduced and has shifted more laterally in prosauropods (Walker 1977; Bonnan 2001). In sauropods, the roughened lateral bulge that landmark 9 demarcates is assumed here to be homologous to the lesser trochanter of other saurischians (see Bonnan 2001 for a more detailed consideration of this landmark). If M. iliofemoralis inserted on this landmark in sauropods, the more proximal location of the lesser trochanter in *Diplodocus*, and its more distal location in *Apatosaurus* and *Camarasaurus*, suggests a difference in femoral protraction (see below).

Assuming the femur was columnar and had limited long-axis rotation, and that its motion prescribed a parasagittal arc, the following inferences regarding functional morphology are drawn from the thin-plate splines results. For all three sauropods, the combined action of the M. caudofemorales on the femur would act as the in-force of a second-order lever system. Here, as with the deltopectoral system described above for the humerus, the femoral head is the fulcrum and the femoral shaft is the out-lever. The more distally placed the fourth trochanter is from the femoral head, the greater the turning moment of the femoral shaft about the femoral head becomes while

simultaneously decreasing the arc of femoral retraction (see Hildebrand and Goslow 2001: Fig. 24.8 for a diagram of this specific changing mechanical relationship). In *Diplodocus*, the more proximal placement of the fourth trochanter would place the in-force of the M. caudofemorales closer to the femoral head. This would act to increase the arc of the femoral shaft during retraction but would decrease femoral torque. In contrast, the more distal fourth trochanter placement in *Apatosaurus* and *Camarasaurus* suggests increased torque but a reduced arc of femoral retraction compared with *Diplodocus*.

Assuming M. iliofemoralis inserted into the lesser trochanter (landmark 9) in the three sauropods, the distance of this landmark from the femoral head would affect the leverage of this muscle on the femur. The columnar orientation of the femur would limit the action of M. iliofemoralis mostly to stabilizing the femoral head against the acetabulum (see Walker 1977 for a discussion of this function in all dinosaurs). Some degree of femoral protraction was also likely (see Bonnan 2001 for further discussion), but for simplicity only the inferred stabilizing action of M. iliofemoralis will be considered here. Again, as with the fourth trochanter, M. iliofemoralis would act as the in-force in a second-order lever system. In this case, without considering femoral protraction, the force (torque) holding the femoral head against the acetabulum would increase as the lesser trochanter moved distally. The more distal placement of the lesser trochanter in *Apatosaurus* and *Camarasaurus* femora suggests a greater stabilizing force than would be predicted for the *Diplodocus* femur where this landmark is more proximal.

Functional Summary and Locomotor Implications

The results of the statistical analyses and the inferred functional differences among the three sauropod taxa can be summarized as follows. Humeri of all three sauropods typically show isometric dimensional changes with increased size. The *Apatosaurus* humerus is clearly different from those of *Diplodocus* and *Camarasaurus* in being a robust element characterized by mediolateral expansion, an elongated deltopectoral crest, and an enlarged medial ''epicondyle.'' In contrast, *Diplodocus* and *Camarasaurus* have a more gracile humerus with reduced proximal and distal ends and a more proximally terminating deltopectoral crest. By EPB comparison, the stabilizing M. subcoracoscapularis and the humeral flexor M. supracoracoideus probably inserted into the medial and lateral regions of the proximal end of the humerus, respectively, whereas deltopectoral muscles would have inserted along the deltopectoral crest. Interpreted as a second-order lever system, the more elongate deltopectoral crest in *Apatosaurus* suggests that the in-force of its deltopectoral muscles was shifted more distally than in the other taxa, increasing the torque of the humerus about its head but decreasing its arc of flexion. An opposite trend is inferred for *Diplodocus* and *Camarasaurus*. The enlarged medial ''epicondyle'' of *Apatosaurus* may be tied with the flexors of its robust manus and pollex claw.

Femora of all three taxa show an overall isometric trend with increased size, with moderately negative allometric trends in mediolateral expansion for *Camarasaurus* and positive allometry for the proximal end of the *Diplodocus* femur. Linear measurement data show again that *Apatosaurus* femora are more robust than those of *Diplodocus* and *Camarasaurus*. For all taxa, the midshaft dimensions of the femur appear to expand more mediolaterally than anteroposteriorly as element size increases. This midshaft allometry suggests that retention of an oval femoral cross-section served an important biomechanical function such as resistance of mediolateral shear (e.g., Wilson and Sereno 1998). Morphologically, the femur of *Diplodocus* is clearly different from those of *Apatosaurus* and *Camarasaurus* in being more gracile and in having more proximal fourth and lesser trochanters. EPB comparison suggests that these landmarks served as the attachment sites for femoral retractors (M. caudofemorales) and a stabilizer of the femur (M. iliofemoralis), respectively. According to the principles of a second-order lever system, the more proximally situated fourth trochanter of *Diplodocus* suggests an increased range of femoral retraction with decreased torque about the femoral head.

An inverse trend is predicted for *Apatosaurus* and *Camarasaurus*. The more proximal location of the lesser trochanter in *Diplodocus* suggests less torque about the femoral head than for the other taxa.

The robust humeri and femora of *Apatosaurus* and their expanded or more distally placed muscle insertion regions and landmarks reflect the overall massiveness of the skeleton. The statistical results and functional inferences reported here suggest that *Apatosaurus* had powerful humeral protractors and femoral retractors, but a smaller range of humeral flexion than *Diplodocus* and *Camarasaurus* and a smaller range of femoral extension than *Diplodocus*. If the expansion of its medial ''epicondyle'' reflects the possession of more powerful manus and pollex claw flexors, the contribution of the manus to locomotion (e.g., flexing during propulsion, pollex claw engagement of the substrate) may have been greater in *Apatosaurus* than in the other genera. The elongate humerus and femur of *Diplodocus*, the more proximally placed insertion sites for protractors and retractors, and its ''light'' skeleton (e.g., McIntosh 1990; Paul 1997) all suggest that this sauropod had the longest stride of the three genera. The locomotor ''scope'' of *Camarasaurus* falls somewhere between that of *Apatosaurus* and *Diplodocus*: the more gracile humerus with its more proximally situated deltopectoral crest suggests a range of parasagittal flexion similar to that of *Diplodocus*, whereas the more robust femur with its more distal fourth trochanter would provide a shorter but more powerful range of extension more akin to *Apatosaurus*.

Surprisingly few differences were detected between adult and juvenile specimens using both the traditional and thin-plate splines techniques. For the humerus, no discernible differences were detected between juveniles and adults in any of the three taxa. One juvenile *Apatosaurus* femur did cluster with adult *Diplodocus* specimens in the relative warps analysis. The juvenile *Apatosaurus* specimen (CM 566) is gracile and has more proximally situated fourth and lesser trochanters, a morphology similar to that of adult *Diplodocus* specimens. This morphological convergence is interesting but a larger sample of juvenile and adult elements is necessary to clarify whether this is indeed a real biological signal. The similarities between the single *Apatosaurus* specimen and the *Diplodocus* femora tentatively suggest that the two genera had morphologically similar femora as juveniles but followed different shape trajectories during ontogeny.

The morphological differences in the humeri and femora detected among the three genera are not surprising given that these sauropods differ from one another in skull, dental, and cervical morphology. The narrow skulls, pencil-like teeth, reduced dental microwear (Fiorillo 1991; Calvo 1994), long necks, and inferred strip-feeding behavior of *Apatosaurus* and *Diplodocus* suggested to Upchurch and Barrett (2000) that these sauropods were selective feeders. In contrast, the robust skull, spatulate teeth, and the anteroposteriorly expanded jaw joint of *Camarasaurus* suggest that this sauropod incorporated heavy shearing and moderate propalinial motions in its feeding (Upchurch and Barrett 2000). As Fiorillo (1991) and Calvo (1994) discovered, more microwear was present on *Camarasaurus* teeth than those of *Diplodocus*, which suggested a diet of coarser vegetation and ingestion of more grit in this genus. The necks of *Apatosaurus* and *Diplodocus* apparently had limited dorsiflexion, were typically held in a horizontal orientation, and had well-developed ventriflexion (Stevens and Parrish 1997, 1999), characteristics that suggest both sauropods were low browsers, using their horizontal necks as sweeping feeding booms. The range of cervical dorsiflexion in *Camarasaurus* remains unclear (Parrish and Stevens 1998), but this sauropod may have had a greater vertical feeding range than the diplodocids.

Drawing paleoecological inferences from limb morphology is several levels removed from the primary osteology (e.g., the inference pyramid of Witmer 1995), and data on the shape and articulation of the feet and lower limb elements were not considered in the present study. Therefore, paleoecological interpretations of limb differences are beyond the scope of this analysis. However, several paleoecological questions are raised from the mor-

phological data. Recent Late Jurassic paleobotanical data suggest that the large conifers and ginkgoes that formed the bulk of the canopy were both relatively sparse and nutrient poor (Miller 1987; Ash and Tidwell 1998; Chin and Kirkland 1998; Demko and Parrish 1998). In the Morrison, the major low-growing biomass consisted of ferns, horsetails, cycadeoids, seed ferns, and other gymnosperms, pteridophytes, and bryophytes (Miller 1987; Ash and Tidwell 1998; Demko and Parrish 1998). All extant ferns, horsetails, and bryophytes require a wet cycle in order to reproduce (Foster and Gifford 1974), and it seems most parsimonious that their Late Jurassic ancestors had similar reproductive strategies. Thus, feeding on such low-growing vegetation may have necessarily involved traversing damp or muddy substrates. If *Apatosaurus* and *Diplodocus* were both low browsers, what potential advantages would be incurred from robust or gracile humeri and femora if walking on wet sediments? What are the locomotor implications of the differences between humerus and femur morphology in *Camarasaurus*? If *Camarasaurus* had a greater vertical feeding range, would the differences between its autopodial and propodial morphology be tied with walking on more variable terrain than the diplodocids? These questions and others await analyses of the lower limb elements and feet in these and other sauropods.

Conclusions

Both traditional morphometric methods and thin-plate splines revealed paleobiological trends among the humeri and femora of *Apatosaurus*, *Diplodocus*, and *Camarasaurus*. Principal components analysis, linear regression, and bivariate plots of linear measurement variables revealed mostly size-related trends among the taxa. That size accounted for most of the sample variation in the PCAs and bivariate analyses appears to reflect the gross difference in size between the smallest and largest individuals in the sample. The results reported here correlate with previous analyses of sauropod limb dimensions. Perhaps the most significant result gained from analysis of the linear measurement variables is the isometric relationship of most humeral and femoral dimensions to size, bolstering suggestions by Wilhite and Curtice (1998) and Wilhite (1999) that sauropod ontogeny was isometric. Size differences, preservational considerations (e.g., loss of epiphyseal morphology during fossilization), or some hitherto unexamined or unknown biological phenomena might explain these weak allometric trends.

Although linear measurement data revealed broad size-related trends among sauropod taxa, their ability to elucidate finer-scale morphological trends was limited. Thin-plate splines were more effective in revealing underlying shape-based patterns in the humerus and femur, and were a particularly useful morphometric tool for exploring sauropod appendicular functional morphology because they provided both statistical and visual data. Thin-plate splines revealed significant, shape-specific differences that were not detected with traditional methods: the expanded medial ''epicondyle'' of the *Apatosaurus* humerus, the more gracile humerus of *Camarasaurus*, the more proximal location of the fourth and lesser trochanters in *Diplodocus*, and possible similarities in shape between juvenile *Apatosaurus* and *Diplodocus* femora.

Overall, the morphometric results suggest *Apatosaurus*, *Diplodocus*, and *Camarasaurus* have significant morphological differences in their humeri and femora that may be correlated with differences in locomotor functional morphology. Future exploration and quantification of the appendicular skeleton is necessary to complete the paleobiological and paleoecological picture of these giant herbivores. Furthermore, the results of this study suggest that a concerted effort to combine traditional measures of bone dimensions with newer shape-based approaches of sauropod postcrania is likely to yield more informative morphological and paleobiological data than with traditional approaches alone. A distinct advantage of using a shape-based morphometric tool such as thin-plate splines is that it allows one to root functional morphology within a repeatable statistical framework. It is stressed that thin-plate splines and other shape analysis methods should not replace, but complement, traditional morphometric approaches. Perhaps, as in this study, a tech-

nique such as thin-plate splines would be used to elucidate finer-scale morphometric signals, while traditional morphometrics served to highlight large-scale patterns. Ultimately, the use of traditional and shape-based morphometric analyses, in combination with EPB analysis and comparative anatomical studies, strengthens inferences regarding sauropod paleobiology and evolution.

Acknowledgments

The work presented here is derived, in part, from a dissertation on sauropod locomotion completed under J. M. Parrish at Northern Illinois University (NIU). I wish to extend my thanks to J. M. Parrish and the members of my dissertation committee for their help and discussions on the initial analysis of these data: N. Blackstone, D. Gebo, W. Hammer, and V. L. Naples. The comments and suggestions of two anonymous reviewers on an earlier draft of this paper improved the final manuscript. I thank J. Farlow and an anonymous reviewer for their helpful suggestions and corrections. R. Chapman, R. King, S. Meagher, and M. Romano provided helpful statistical advice. R. Wilhite kindly provided the author with a copy of his Master's thesis. R. Elsey of the Louisiana Rockefeller Wildlife Refuge generously provided *Alligator* specimens for dissection. I am thankful for the hospitality and assistance of curators and staff at all museums I have visited for help with some very heavy bones (see Appendix 1 for institutional names): E. Gaffney and staff (AMNH); K. Stadtman (BYU); D. Burge and staff (CEU); D. Berman, B. Hill, and staff (CM); D. Chure (DNM); W. Simpson, B. Stanley, and staff (FMNH); Staff (HMNS); L. Martin and staff (KUVP); B. Britt and R. Scheetz (MWC); M. K. Brett-Surman, B. Purdy, R. Chapman, and staff (NMNH); R. Cifelli, M. Wedel, and staff (OMNH); B. Wahl and staff (TATE); D. and J. Gillette (UMNH); C. Chandler, M. A. Turner, and staff (YPM). This research was supported by two American Museum of Natural History Theodore Roosevelt Memorial Grants, a Sigma-Xi Grant-in-Aid-of-Research, J. Kirkland and the Dinamation International Society, a Dissertation Completion Fellowship at NIU, and the Department of Biological Sciences at Western Illinois University.

Literature Cited

Alexander, R. M. 1989. Dynamics of dinosaurs and other extinct giants. Columbia University Press, New York.

Alexander, R. M., and A. S. Jayes. 1983. A dynamic similarity hypothesis for the gaits of quadrupedal mammals. Journal of Zoology, London 201:135–152.

Ash, S. R., and W. D. Tidwell. 1998. Plant megafossils from the Brushy Basin Member of the Morrison Formation near Montezuma Creek Trading Post, Southeastern Utah. Modern Geology 22:321–339.

Benton, M. J. 1997. Origin and early evolution of dinosaurs. Pp. 204–215 *in* Farlow and Brett-Surman 1997.

Birch, J. M. 1997. Comparing wing shape of bats: the merits of principal-components analysis and relative-warp analysis. Journal of Mammalogy 78:1187–1198.

Bonnan, M. F. 2001. The evolution and functional morphology of sauropod dinosaur locomotion. Ph.D. dissertation. Northern Illinois University, DeKalb.

———. 2003. The evolution of manus shape in sauropod dinosaurs: implications for functional morphology, forelimb orientation, and phylogeny. Journal of Vertebrate Paleontology 23:595–613.

Bookstein, F. L. 1990. Higher-order features of shape change for landmark data. Pp. 237–250 *in* F. J. Rohlf and F. L. Bookstein, eds. Proceedings of the Michigan Morphometrics Workshop. University of Michigan Museum of Zoology, Ann Arbor.

———. 1991. Morphometric tools for landmark data: geometry and biology. Cambridge University Press, New York.

———. 1996. Combining the tools of geometric morphometrics. Pp. 131–151 *in* L. F. Marcus, M. Corti, A. Loy, G. J. P. Naylor, and D. E. Slice, eds. Advances in morphometrics. Plenum, New York.

Bookstein, F. L., B. Chernoff, R. Elder, J. Humphries, G. Smith, and R. Strauss. 1985. Morphometrics in evolutionary biology. Special Publication No. 15. Academy of Natural Sciences, Philadelphia.

Calvo, J. O. 1994. Jaw mechanics in sauropod dinosaurs. GAIA 10:183–193.

Carpenter, K., and P. J. Currie, eds. 1990. Dinosaur systematics: perspectives and approaches. Cambridge University Press, New York.

Carrano, M. T. 1997. Mammals versus birds as models for dinosaur limb kinematics. Journal of Vertebrate Paleontology 17(Suppl. to No. 3):36A.

———. 1998. Locomotion in non-avian dinosaurs: integrating data from hindlimb kinematics, in vivo strains, and bone morphology. Paleobiology 24:450–469.

———. 1999. What, if anything, is a cursor? Categories versus continua for determining locomotor habit in mammals and dinosaurs. Journal of Zoology 247:29–42.

Chapman, R. E. 1990a. Shape analysis in the study of dinosaur morphology. Pp. 21–42 *in* Carpenter and Currie 1990.

———. 1990b. Conventional Procrustes approaches. Pp. 251–267 *in* F. J. Rohlf and F. L. Bookstein, eds. Proceedings of the Michigan Morphometrics Workshop. University of Michigan Museum of Zoology, Ann Arbor.

———. 1997. Technology and the study of dinosaurs. Pp. 112–135 *in* Farlow and Brett-Surman 1997.

Chapman, R. E., and D. B. Weishampel. 1997a. Biometrics. Pp. 59–62 *in* P. J. Currie and K. Padian, eds. Encyclopedia of dinosaurs. Academic Press, New York.

———. 1997b. Computers and related technology. Pp. 137–142 *in* P. J. Currie and K. Padian, eds. Encyclopedia of dinosaurs. Academic Press, New York.

Chin, K., and J. I. Kirkland. 1998. Probable herbivore coprolites from the Upper Jurassic Mygatt-Moore Quarry, Western Colorado. Modern Geology 22:249–275.

Christiansen, P. 1997. Locomotion in sauropod dinosaurs. GAIA 14:45–75.
Coombs, W. P. 1978. Theoretical aspects of cursorial adaptations in dinosaurs. Quarterly Review of Biology 53(12):393–418.
Curry, K. A. 1999. Ontogenetic history of *Apatosaurus* (Dinosauria: Sauropoda): new insights on growth rates and longevity. Journal of Vertebrate Paleontology 19:654–665.
Curtice, B. D., J. R. Foster, and D. R. Wilhite. 1997. A statistical analysis of sauropod limb elements. Journal of Vertebrate Paleontology 17(Suppl. to No. 3):41A.
Demko, T. M., and J. T. Parrish. 1998. Paleoclimatic setting of the Upper Jurassic Morrison Formation. Modern Geology 22:283–296.
Dodson, P. 1990. Sauropod paleoecology. Pp. 402–407 *in* D. B. Weishampel, P. Dodson, and H. Osmólska, eds. The Dinosauria. University of California Press, Berkeley.
Dodson, P., A. K. Behrensmeyer, R. T. Bakker, and J. S. McIntosh. 1980. Taphonomy and paleoecology of the dinosaur beds of the Jurassic Morrison Formation. Paleobiology 6:208–232.
Farlow, J. O., and M. K. Brett-Surman, eds. 1997. The complete dinosaur. Indiana University Press, Bloomington.
Farlow, J. O., S. M. Gatesy, T. R. Holtz, J. R. Hutchinson, and J. M. Robinson. 2000. Theropod locomotion. American Zoologist 40:640–663.
Fiorillo, A. R. 1991. Paleoecological inferences based on the dental microwear patterns on the teeth of *Camarasaurus* and *Diplodocus*. Journal of Vertebrate Paleontology 11(Suppl. to No. 3):28A.
Foster, A. S., and E. M. Gifford. 1974. Comparative morphology of vascular plants, 2d ed. W. H. Freeman, San Francisco.
Foster, J. R. 1995. Allometric and taxonomic limb bone robustness variability in some sauropod dinosaurs. Journal of Vertebrate Paleontology 15(Suppl. to No. 3):29A.
Gatesy, S. M. 1990. Caudofemoral musculature and the evolution of theropod locomotion. Paleobiology 16:170–186.
———. 1995. Functional evolution of the hindlimb and tail from basal theropods to birds. Pp. 219–234 *in* J. J. Thomason, ed. Functional morphology in vertebrate paleontology. Cambridge University Press, New York.
———. 1997. An electromyographic analysis of hindlimb function in *Alligator* during terrestrial locomotion. Journal of Morphology 234:197–212.
———. 1999. Guineafowl hind limb function. II. Electromyographic analysis and motor pattern evolution. Journal of Morphology 240:127–142.
Gatesy, S. M., and K. M. Middleton. 1997. Bipedalism, flight, and the evolution of theropod locomotor diversity. Journal of Vertebrate Palaeontology 17:308–315.
George, J. C., and A. J. Berger. 1966. Avian myology. Academic Press, New York.
Haines, R. W. 1942. The evolution of epiphyses and endochondral bone. Biological Reviews 17:267–292.
Hildebrand, M., and G. Goslow. 2001. Analysis of vertebrate structure, 5th ed. Wiley, New York.
Horner, J. R., K. Padian, and A. de Ricqlès. 2001. Comparative osteohistology of some embryonic and perinatal archosaurs: developmental and behavioral implications for dinosaurs. Paleobiology 27:39–58.
Jolicoeur, P. 1963. The multivariate generalization of the allometry equation. Biometrics 19:497–499.
Jones, T. D., J. O. Farlow, J. A. Ruben., D. M. Henderson, and W. J. Hillenius. 2000. Cursoriality in bipedal archosaurs. Nature 406:716–718.
Lehman, T. M. 1990. The ceratopsian subfamily Chasmosaurinae: sexual dimorphism and systematics. Pp. 211–229 *in* Carpenter and Currie 1990.
Liem, K. F., W. E. Bemis, W. F. Walker, and L. Grande. 2001. Functional anatomy of the vertebrates, 3d ed. Harcourt College Publishers, New York.
MacLeod, N. 1999. Generalizing and extending the eigenshape method of shape visualization and analysis. Paleobiology 25: 107–138.
———. 2002. Phylogenetic signals in morphometric data. Pp. 100–138 *in* N. MacLeod and P. L. Forey, eds. Morphology, shape, and phylogeny. Taylor and Francis, NY.
McIntosh, J. S. 1990. Sauropoda. Pp. 345–401 *in* D. B. Weishampel, P. Dodson, and H. Osmólska, eds. The Dinosauria. University of California Press, Berkeley.
McIntosh, J. S., M. K. Brett-Surman, and J. O. Farlow. 1997. Sauropods. Pp. 264–290 *in* Farlow and Brett-Surman 1997.
Miller, C. N. 1987. Land plants of the Northern Rocky Mountains before the appearance of flowering plants. Annals of Missouri Botanical Gardens 74:692–706.
Monterio, L. R. 1999. Functional and historical determinants of shape in the scapula of Xenarthran mammals: evolution of a complex morphological structure. Journal of Morphology 24: 251–263.
Ostrom, J. H., and J. S. McIntosh. 1966. Marsh's dinosaurs. Yale University Press, New Haven, Conn.
Parrish, J. M., and K. A. Stevens. 1998. Undoing the death pose: using computer imaging to restore the posture of articulated dinosaur skeletons. Journal of Vertebrate Paleontology 18(Suppl. to No. 3):69A.
Paul, G. S. 1997. Dinosaur models: the good, the bad, and using them to estimate the mass of dinosaurs; pp. 129–154 *in* D. L. Wolberg, E. Stump, and G. D. Rosenburg, eds. Dinofest International: proceedings of a symposium held at Arizona State University. Academy of Natural Sciences, Philadelphia.
Proctor, N. S., and P. J. Lynch. 1993. Manual of ornithology: avian structure and function. Yale University Press, New Haven, Conn.
Reese, A. M. 1915. The alligator and its allies. G. P. Putnam's Sons, New York.
Rohlf, F. J. 1993. Relative Warp Analysis and an example of its application to mosquito wings. Pp. 131–159 *in* L. F. Marcus, E. Bello, and A. Garcia-Valdescasas, eds. Contributions to morphometrics. CSIC, Madrid.
———. 1997a. TPSDIG (Thin Plate Splines Digitizing Software). http://life.bio.sunysb.edu/morph/
———. 1997b. Relative warps (TPSRW), Version 1.6. http://life.bio.sunysb.edu/morph/
———. 1998. On applications of geometric morphometrics to studies of ontogeny and phylogeny. Systematic Biology 47: 147–158.
Rohlf, F. J., and D. E. Slice. 1990. Extensions of the Procrustes method for the optimal superimposition of landmarks. Systematic Zoology 39:40–59.
Romer, A. S. 1923a. Crocodilian pelvic muscles and their avian and reptilian homologues. Bulletin of the American Museum of Natural History 48:533–552.
———. 1923b. The pelvic muscles of saurischian dinosaurs. Bulletin of the American Museum of Natural History 48:605–617.
———. 1956. Osteology of the reptiles. University of Chicago Press, Chicago.
———. 1962. The vertebrate body, 3d ed. W. B. Saunders, Philadelphia.
Sereno, P. C. 1999. The evolution of dinosaurs. Science 284:2137–2147.
Shea, B. T. 1985. Bivariate and multivariate growth allometry: statistical and biological considerations. Journal of Zoology, London A 206:367–390.
Stevens, J. 1996. Applied multivariate statistics for the social sciences, 3d ed. Lawrence Earlbaum, Mahwah, NJ.
Stevens, K. A., and J. M. Parrish. 1997. Comparisons of neck

form and function in the Diplodocidae. Journal of Vertebrate Paleontology 17(Suppl. to No. 3):79A.
———. 1999. Neck posture and feeding habits of two Jurassic sauropod dinosaurs. Science 284:798–800.
Strauss, R. E., M. N. Atanassov, and J. Alves de Oliveira. 2003. Evaluation of the principal-component and expectation-maximization methods for estimating missing data in morphometric studies. Journal of Vertebrate Paleontology 23:284–296.
Swiderski, D. L. 1993. Morphological evolution of the scapula in tree squirrels, chipmunks, and ground squirrels (Sciuridae): an analysis using thin-plate splines. Evolution 47:1854–1873.
Thulborn, R. A. 1989. The gaits of dinosaurs. Pp. 39–50 *in* D. D. Gillette and M. G. Lockley, eds. Dinosaur tracks and traces. Cambridge University Press, New York.
Upchurch, P. 1994. Manus claw function in sauropod dinosaurs. GAIA 10:161–171.
———. 1995. The evolutionary history of sauropod dinosaurs. Philosophical Transactions of the Royal Society of London B 349:365–390.
———. 1998. The phylogenetic relationships of sauropod dinosaurs. Zoological Journal of the Linnean Society 124:43–103.
Upchurch, P., and P. M. Barrett. 2000. The evolution of sauropod feeding mechanisms. Pp. 79–122 *in* H.-D. Sues, ed. Evolution of herbivory in terrestrial vertebrates: perspectives from the fossil record. Cambridge University Press, New York.
Walker, A. D. 1977. Evolution of the pelvis in birds and dinosaurs. Pp. 319–358 *in* S. M. Andrews, R. S. Miles, and A. D. Walker, eds. Problems in vertebrate evolution. Linnean Society Symposium Series 4.
Weishampel, D. B., and R. E. Chapman. 1990. Morphometric study of *Plateosaurus* from Trossingen (Baden-Wurtemberg, Federal Republic of Germany). Pp. 43–51 *in* Carpenter and Currie 1990.
Wilhite, R. 1999. Ontogenetic variation in the appendicular skeleton of the genus *Camarasaurus*. Master's thesis. Brigham Young University, Provo, Utah.
———. 2003. Biomechanical reconstruction of the appendicular skeleton in three North American Jurassic sauropods. Ph.D. dissertation. Louisiana State University, Baton Rouge.
Wilhite, R., and B. Curtice. 1998. Ontogenetic variation in sauropod dinosaurs. Journal of Vertebrate Paleontology 18(Suppl. to No. 3):86A.
Wilson, J. A. 2002. Sauropod dinosaur phylogeny: critique and cladistic analysis. Zoological Journal of the Linnean Society 136:217–276.
Wilson, J. A., and P. C. Sereno. 1998. Early evolution and higher-level phylogeny of sauropod dinosaurs. Journal of Vertebrate Paleontology Memoir 5:1–68.
Witmer, L. M. 1995. The Extant Phylogenetic Bracket and the importance of reconstructing soft tissues in fossils. Pp. 19–33 *in* J. J. Thomason, ed. Functional morphology in vertebrate paleontology. Cambridge University Press, New York.
Zelditch, M. L., W. L. Fink, and D. L. Swiderski. 1995. Morphometrics, homology, and phylogenetics: quantified characters as synapomorphies. Systematic Biology 44:179–189.
Zelditch, M. L., W. L. Fink, and B. L. Lundrigan. 1998. On applications of geometric morphometrics to studies of ontogeny and phylogeny: a reply to Rohlf. Systematic Biology 47:159–167.

Appendix 1

Institutional and Specimen Data

Institutional Abbreviations: AMNH (American Museum of Natural History); BYU (Brigham Young University); CEU (College of Eastern Utah, Price); CM (Carnegie Museum of Natural History); DNM (Dinosaur National Monument); FMNH (Field Museum of Natural History); HMNS (Houston Museum of Natural Science); KUVP (University of Kansas Vertebrate Paleontology Museum); MWC (Museum of Western Colorado); NMNH (National Museum of Natural History); OMNH (Oklahoma Museum of Natural History); TATE (Tate Geological Museum); UMNH (Utah Museum of Natural History); YPM (Yale Peabody Museum).

Appendix 2

Variable abbreviations used in the text.

Element	Variable	Description
Humerus	H1	Maximum length
	H2	Proximal breadth
	H3	Deltopectoral crest length
	H4	Anteroposterior midshaft width
	H5	Mediolateral midshaft width
	H6	Distal breadth
	H7	Lateral ''condyle'' breadth
	H8	Medial ''condyle'' breadth
	H9	Olecranon fossa breadth
	H10	Olecranon fossa height
Femur	F1	Maximum length
	F2	Proximal breadth
	F3	Femoral head breadth
	F4	Greater trochanter breadth
	F5	Distance of fourth trochanter from femoral head
	F6	Distance of fourth trochanter from lateral side of femur
	F7	Distal breadth
	F8	Crural extensor fossa breadth
	F9	Crural extensor fossa height
	F10	Lateral condyle breadth
	F11	Medial condyle breadth
	F12	Anteroposterior midshaft width
	F13	Mediolateral midshaft width